



**BETTER SHIPS, BLUE OCEANS**

## **Effect of speed reduction on underwater radiated noise of ships sailing on the Dutch North Sea**

Report No. : 77002-3-RD  
Date : March 2025  
Version : 2.0  
Final Report

# Effect of speed reduction on underwater radiated noise of ships sailing on the Dutch North Sea

MARIN order No. : 77002.700  
MARIN Project Manager : Johan Bosschers

Number of pages : 46

Ordered by : Ministry of Infrastructure and Water Management  
Directorate-General for Aviation and Maritime Affairs  
Rijnstraat 8  
2515 XP The Hague  
The Netherlands

Reported by : Fernanda dos Santos, Johan Bosschers, Thomas Lloyd, Marjolein Hermans  
Reviewed by : Thomas Lloyd, Johan Bosschers

Version	Date	Version description
0.1	14-12-2024	First draft
1.0	19-12-2024	Updated draft distributed to I&W
2.0	28-02-2025	Final

<b>CONTENTS</b>	<b>PAGE</b>
REVIEW OF TABLES AND FIGURES .....	III
MANAGEMENT SUMMARY .....	V
1 INTRODUCTION.....	1
2 DATASET AND STATISTICAL DISTRIBUTION OF SHIPS AND SAILING SPEED IN THE NORTH SEA .....	3
2.1 Dataset .....	3
2.2 Vessel categories .....	4
2.3 Distribution of ships in the North Sea .....	5
2.4 Statistical distribution of speed over ground in the North Sea .....	5
3 STATISTICAL DISTRIBUTION OF THE CAVITATION INCEPTION SPEED AND SERVICE SPEED OF VESSELS SAILING IN THE NORTH SEA .....	8
3.1 Service speed .....	8
3.2 Cavitation inception speed .....	11
4 SOUND LEVEL ESTIMATION FOR VESSELS SAILING IN THE NORTH SEA AND THE EFFECT OF SLOWDOWN .....	14
4.1 Prediction models for the radiated noise levels.....	14
4.1.1 J-E model.....	14
4.1.2 ECHO-RNL model .....	16
4.1.3 Comparison of the radiated noise level spectra for the J-E and ECHO-RNL models ..	17
4.2 Slowdown analysis and effect .....	19
4.2.1 Cumulative density distribution of the radiated noise level.....	19
4.2.2 Radiated noise exposure level .....	21
4.2.3 Sensitivity of the results for the slow container vessels .....	24
4.2.4 Journey time .....	25
5 CONCLUSIONS.....	28
BIBLIOGRAPHY .....	30
APPENDIX 1 .....	A1.1

## REVIEW OF TABLES AND FIGURES

### Tables:

Table 2-1 -	Ships categories considered in this study. ....	4
Table 2-2 -	Average SOG based on the average SOG per journey and the standard deviation for each ship type. ....	7
Table 3-1 -	Average block coefficient for each vessel category. ....	13
Table 4-1 -	Difference of the mean RNL values between the slowdown and reference case for RNL estimates based on the J-E model and on the ECHO-RNL model for two decedecade frequency bands. Negative values indicate a reduction of the RNLs for the slowdown case. ....	21
Table 4-2 -	Average journey time with and without applying the slowdown, difference between the average journey times (journey delay), and average SOG without considering the slowdown. ....	26
Table A1-1 -	ORNEL and <i>ORN<sub>Lavg</sub></i> (overall <i>RNL<sub>Lavg</sub></i> ) based on the estimates from the J-E model for the reference and slowdown cases. The overall level was calculated for decedecade bands from 20 Hz to 20 kHz. ....	7
Table A1-2 -	ORNEL and <i>RNL<sub>Lavg</sub></i> (overall <i>RNL<sub>Lavg</sub></i> ) based on the estimates from the ECHO-RNL model for the reference and slowdown cases. The overall level was calculated for decedecade bands from 20 Hz to 20 kHz. ....	7

### Figures:

Figure 1-1 -	Radiated noise level for a 173-m merchant vessel for different ship speeds. Adapted from (Arveson and Vendittis 2000). ....	1
Figure 1-2 -	Left: Example of machinery and propeller cavitation noise scaling with ship speed for a specific vessel. Right: Power of the speed scaling for the J-E model and the ECHO-RNL model. J-E model considers a speed scaling to the sixth power for all ship types and frequencies, whereas the ECHO-RNL model considers the speed scaling dependency on frequency and ship type. ....	2
Figure 2-1 -	Area selected in the North Sea (green area) where the AIS data was extracted for the year 2023. ....	3
Figure 2-2 -	Normalised number of unique vessels, normalised number of journeys and number of journeys per number of unique vessels for 2023 for the North Sea area selected. ....	5
Figure 2-3 -	Probability density distribution of the average speed over ground per journey for each ship type. Bin width of 2 kn. A Gaussian distribution based on the mean and standard deviation of the speed over ground is also included. The red-dashed line indicates the speed limit set in the ECHO Program of voluntary vessel slowdown. ....	7
Figure 3-1 -	Comparison of the service speed from the Significant Ships dataset and the formulations available to estimate the service for different ship categories. ....	9
Figure 3-2 -	Service speed as a function of the ship length overall. ....	10
Figure 3-3 -	Probability density distribution of the speed over ground normalised by the service speed per ship type. Bin width of 0.05. ....	11
Figure 3-4 -	Comparison of the block coefficient from the Significant Ships dataset with the formulation available to estimate the block coefficient (Eq. 6) for different ship categories. The <i>x</i> -axis show the ship number given to each vessel in the dataset. ....	12
Figure 3-5 -	Probability density distribution of the speed over ground normalised by the service speed per ship type. Bin width of 0.05. ....	13
Figure 4-1 -	Left: schematic of the Lloyd's mirror effect in the context of the ship sound measurement. Right: Lloyd's mirror correction as a function of <i>f</i> for <i>d</i> = 10 m. ....	16
Figure 4-2 -	Mean radiated noise level for different ship types and the speed scaling coefficient for the ECHO-RNL model. ....	17
Figure 4-3 -	Radiated noise levels estimated from the J-E model and the ECHO-RNL model for different ship categories. The RNL is estimated for three different conditions (speed over ground (sog) and length overall ( <i>Loa</i> )). These conditions were randomly selected from the dataset. ....	18

Figure 4-4 - Cumulative density distribution of the source levels for each ship category for a centre decade band of 125 Hz for two cases: reference and ECHO slowdown. The source levels are estimated based on the J-E model and the ECHO-RNL model. Bin width of 2 dB. .... 20

Figure 4-5 - Annually average RNL as a function of decade frequency bands for each ship category and for the reference and slowdown cases. The radiated noise levels were estimated based on the J-E model and the ECHO-RNL model. The levels correspond to *RNL<sub>avg</sub>* considering all the data points. .... 22

Figure 4-6 - Difference between the RNEL for the reference and slowdown cases. Negative values indicate a reduction of the RNEL when the slowdown is respected. The radiated noise levels were estimated based on the J-E model and the ECHO-RNL model. .... 23

Figure 4-7 - Difference of the ORNEL between the slowdown (SD) and the reference (ref) cases for each ship type and source level model. The difference is shown for different frequency ranges considered to compute the ORNEL. .... 24

Figure 4-8 - Difference of the ORNEL between the slowdown (SD) and the reference (ref) cases for each ship type and noise estimation model. Each image shows the results for a different threshold speed to differentiate fast containers and bulkers/slow containers and for a speed limit for the slow containers. .... 25

Figure 4-9 - Average journey delay, standard deviation of the journey delay and number of journeys as a function of the journey time without delay for the different ship categories. Absolute and normalised values are presented. The journey time without delay was binned in 15-minute intervals, with the centre value of each bin plotted in the graphs. .... 27

Figure 4-10 - Cumulative density distribution of the journey delay normalised by the journey time without slowdown for the different ship categories. .... 27

Figure A1-1 - Cumulative density distribution of the speed over ground per ship type. Bin width of 2 kn. A Gaussian distribution based on the mean and standard deviation of the speed over ground is also included. The vertical lines indicate the average service speed and inception speed for each vessel type. ....1

Figure A1-2 - Cumulative density distribution of the speed over ground normalised by the service speed per ship type. Bin width of 0.05. ....2

Figure A1-3 - Cumulative density distribution of the speed over ground normalised by the cavitation inception speed per ship type. Bin width of 0.05. ....3

Figure A1-4 - Cumulative density distribution of the source levels for each ship category for a centre decade band of 63 Hz for two cases: reference and ECHO slowdown. The source level is estimated based on the J-E model. Bin width of 2 dB. ....4

Figure A1-5 - Cumulative density distribution of the source levels for each ship category for a centre decade band of 125 Hz for two cases: reference and ECHO slowdown. The source level is estimated based on the J-E model. Bin width of 2 dB. ....5

Figure A1-6 - Cumulative density distribution of the source levels for each ship category for a centre decade band of 63 Hz for two cases: reference and ECHO slowdown. The source levels are estimated based on the J-E model and the ECHO-RNL model. Bin width of 2 dB. ....6

## MANAGEMENT SUMMARY

Underwater radiated noise (URN) from shipping is an important contributor to the noise pollution in the oceans and seas, thereby affecting marine life. An operational measure to reduce the radiated noise of a ship is to slowdown the ship speed, as studied by (Findlay, et al. 2023, Port of Vancouver 2024, Nelissen, Kiraly and Meijer 2022). Typically, the empirical JOMOPANS-ECHO (J-E) source level model (MacGillivray and de Jong 2021) is adopted for these studies which assumes that the noise scales with ship speed to the sixth power. However, in reality this speed scaling depends on the relation between machinery and cavitation noise which varies with ship speed and frequency for each ship. A simplified ship URN model that takes into account the speed scaling dependency on the ship type and frequency is the ECHO Radiated Noise Level (ECHO-RNL) model (Hannay et al., 2019).

In the first part of the policy support study of the current project the effect of a propeller redesign and of speed reduction has been investigated for a specific fast sailing container vessel. For this second part of the study, the main goal is to investigate the effect of speed reduction for wider number of ship types sailing on the Dutch part of the North Sea, making use of the regression relations of the ECHO project, i.e., the J-E model and the ECHO-RNL model. Use has been made of AIS data for a selected part of the Dutch North Sea for the year 2023, combined with a ship database of Lloyds List Intelligence. The speed reduction considered in this study is based on the ECHO Program for voluntary ship slowdown (Port of Vancouver 2024). A statistical analysis of the sailing speeds with respect to service speed and cavitation inception speed has also been performed. By following the speed limits in the ECHO Program, the maximum speed reduction for the fastest ship type (fast container) was around 9.0 kn, with an average reduction of 2.9 kn, and the maximum reduction for the lowest ship type (bulker) was around 6.5 kn with an average reduction of 1.3 kn.

The conclusion of the present study is that in general the slowdown results in lower noise levels, with the reduction depending on the type of vessel and frequency range. Striking differences of the estimated noise level reductions for estimates performed with the J-E model and the ECHO-RNL model have been observed. The calculations based on the J-E model estimated that the Overall Radiated Noise Exposure Level (ORNEL) reduces between 2 dB and 3 dB for bulkers, tankers/LPG carriers, LNG carriers, and slow containers. However, according to the ECHO-RNL model, the slowdown would only reduce the ORNEL by less than 1 dB for these vessel types, increasing to 2 dB when a speed limit of 11 kn is applied to the slow-sailing containers. Fast container ships and vehicle carriers are most affected by the slowdown, with a reduction in ORNEL of 3 dB and 1.7 dB, respectively, according to the estimates using the ECHO-RNL model, whereas the J-E model estimates reductions of 4.5 dB and 3.5 dB, respectively. These results show that the slowdown is more effective for fast sailing ships (fast containers and vehicle carriers). For slow sailing ships (bulkers, tankers/LPGs and slow containers), the slowdown results in a reduction of ORNEL but this reduction is smaller than for the fast sailing ships due to the weaker dependency of the RNL on the ship speed and the lower speed reduction. For these vessels, it is expected that the contribution of machinery noise, that has a lower speed dependency than cavitation noise, is more relevant. According to the ECHO-RNL results, the low-frequency range is the most affected by the slowdown for all vessel types.

The results discussed in this study show the importance of considering the speed scaling in more detail when analysing the benefits of a slowdown program. Still, in the present project the different speed scaling of machinery noise and cavitation noise was not included due to lack of a suitable simple model, although a simple model for cavitation inception speed has been analysed. Therefore, it is important to further develop noise estimation models for this type of investigation, for instance based on (Lloyd, et al. 2024, MacGillivray, Ainsworth, et al. 2022), in order to support the creation of effective measures to reduce underwater radiated noise. Another point for further investigation is the definition of a slow-sailing container vessel and the speed limit that should be applied to this category because these vessels have the largest number of journeys for the selected area of the Dutch North Sea.

## 1 INTRODUCTION

Anthropogenic underwater noise has increased significantly in the last decades and is negatively affecting the marine environment (Duarte, et al. 2021). Shipping noise is recognised as an important contributor to the marine soundscape with effects on marine life, such as changes in behavioural response, masking of communication and echolocation, and stress (Erbe, et al. 2019). Within the International Maritime Organization (IMO), revised guidelines<sup>1</sup> for the reduction of underwater noise from commercial shipping has been approved in July 2023 (MEPC.1/Circ.833) to address the adverse impacts of shipping noise on marine life. To tackle this issue, technical and operational solutions are available. From the technical point of view, the use of low-noise propeller design or air injection can lead to a reduction of underwater noise (Lloyd, et al. 2024). The effect of propeller design in the trade-off of underwater noise and greenhouse gas emissions has been investigated in part one of this study in MARIN report 77002-2-RD. In relation to operational solutions, rerouting and slowdown have shown to be promising measures to reduce underwater noise. Thus, the current report focuses on the effects of slowdown on underwater noise.

Figure 1-1 shows the radiated noise level (RNL) as a function of frequency for four different ship speeds as an example of the effect of reducing ship speed on ship noise. As the speed decreases, the RNL also reduces. However, it does not reduce equally for all frequencies. For example, as the ship speed reduces from 12 kn to 10 kn, a RNL reduction of approximately 6 dB is observed at 100 Hz, but no reduction is observed at 10 kHz.

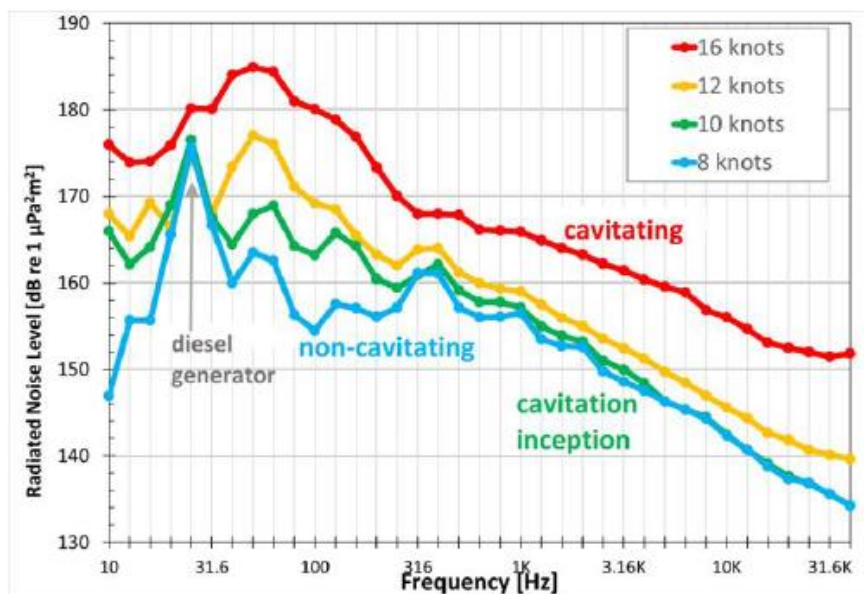


Figure 1-1 - Radiated noise level for a 173-m merchant vessel for different ship speeds. Adapted from (Arveson and Vendittis 2000).

In the study conducted by Findlay et al. (2023), it was assumed that the ship source levels scale with ship speed to the sixth power, which was based on the JOMOPANS-ECHO (J-E) source level (SL) model (MacGillivray and de Jong 2021):

$$L_S [dB] \propto 10 \log_{10}(V_{ship})^6 = 60 \log_{10}(V_{ship}), \text{ for the JE model} \quad \text{Eq. 1}$$

where  $L_S$  is the source level emitted by the ship and  $V_{ship}$  is the ship speed. According to the J-E model, a decrease of speed by a factor of two would result in a decrease of 18 dB. This commonly used scaling is a simplification of the speed scaling for machinery and propeller cavitation noise, as shown in Figure

<sup>1</sup> with respect to 2014.

1-2. However, more recent models (MacGillivray, Ainsworth, et al. 2022, Hannay, et al. 2019) have improved this relation and use a speed scaling that is a function of ship type and frequency.

For example, the power for the speed scaling for the ECHO-RNL model (Hannay, et al. 2019) as a function of frequency is shown in Figure 1-2 for different ship types. The power of the speed scaling for the J-E model is also included, which is constant with frequency. From this figure, it is clear that the sound levels scale with speed to a lower power than assumed in the J-E model. The main differences are for bulkers and tankers, with the power being nearly zero for frequencies around 1 kHz for tankers, and for container ships and vehicle carriers in the mid-frequency range (100 Hz – 1 kHz). Due to the larger power for the speed scaling for the J-E model, the prediction of the source level reduction for the slowdown of vessels will be too optimistic when using this model. This highlights the importance of carefully selecting the source level model when investigating the effect of slowdown on underwater radiated noise (and in general). The frequency range at which the source level is affected due to a slowdown is also important. The attenuation of the sound waves as they propagate is frequency dependent, with low frequencies presenting a lower attenuation. Thus, low-frequency sound (i.e. less than a few hundred Hz) can be heard at much larger distances than high-frequency sound (Ainslie 2010). Moreover, animals have different hearing ranges and auditory frequency weighting functions, which determine the sensitivity of an animal to the sound at specific frequencies. In this way, the relevant frequency range for noise reduction also depends on the species that live in the location of interest (Lucke, et al. 2024, Southall, et al. 2019).

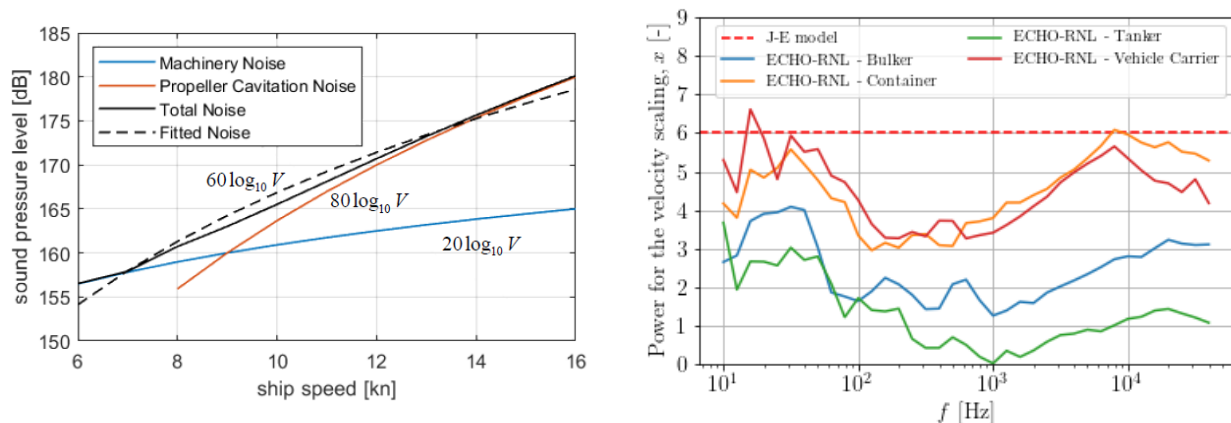


Figure 1-2 - Left: Example of machinery and propeller cavitation noise scaling with ship speed for a specific vessel. Right: Power of the speed scaling for the J-E model and the ECHO-RNL model. J-E model considers a speed scaling to the sixth power for all ship types and frequencies, whereas the ECHO-RNL model considers the speed scaling dependency on frequency and ship type.

In the first part of the I&W study the effect of a propeller redesign and of speed reduction has been investigated for a specific fast sailing container vessel. For the second part of the study, the main goal is to investigate the effect of speed reduction for a limited number of ship types for ships sailing on a selected part of the Dutch North Sea, making use of the regression relations of the ECHO project, i.e., the J-E model (MacGillivray and de Jong 2021) and the ECHO-RNL model (Hannay, et al. 2019). The speed reduction considered in this study is based on the ECHO Program for voluntary ship slowdown (Port of Vancouver 2024). Note that in the NAVISON project (NAVISON 2024), MARIN has developed a detailed ship source model (Lloyd, et al. 2024), which depends on many ship parameters to be obtained from ship databases. For the present study this model can unfortunately not be used as these databases are not in the possession of MARIN. The effect of a propeller redesign can only be investigated for a specific ship of which the hull and propeller geometry is available and as these are not available this is omitted. Furthermore, the statistical distribution of the sailing speed, service speed, and cavitation inception speed for different ship types are analysed for the selected part of the Dutch North Sea.



## 2 DATASET AND STATISTICAL DISTRIBUTION OF SHIPS AND SAILING SPEED IN THE NORTH SEA

In this section, the dataset used to perform the analysis in this study is described in Section 2.1. In Section 2.2, the vessel categories investigated in this study are defined. Afterwards, the number of unique vessels and journeys per ship type for the selected area for a period of one year (2023) are presented in Section 2.3. The statistical distribution of the speed over ground for each ship type is discussed in Section 2.4. The statistical distribution of the ship's service speed, inception speed, and emitted sound are discussed in Chapters 3 and 4.

### 2.1 Dataset

The dataset used in this study was extracted from the automatic identification system (AIS), which is an automatic tracking system that transmits the ship's location, speed over ground (SOG), draught, and other relevant information, which are recorded. The selected area in the Dutch North Sea is highlighted in green in Figure 2-1. This area was selected due to its proximity to the Frisian Islands (Waddeneilanden in Dutch). It encompasses four ship lanes in the Dutch North Sea. The AIS data was extracted for the year of 2023.

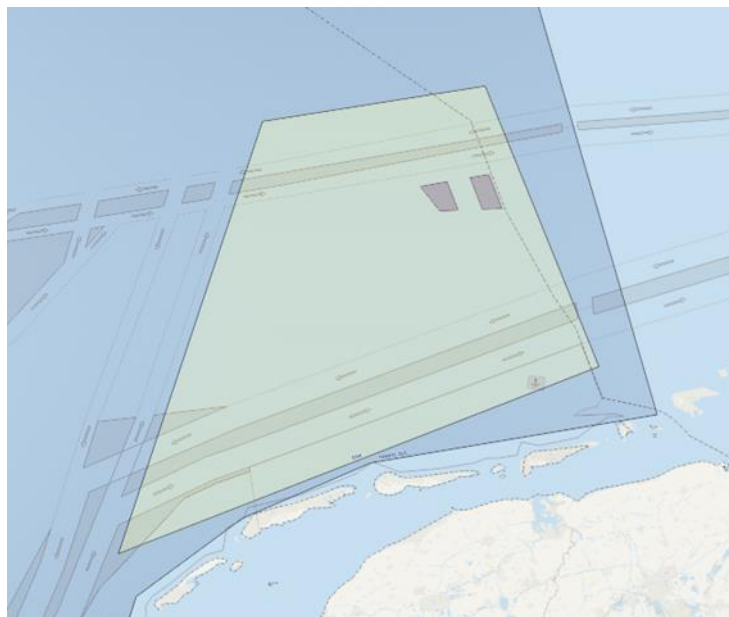


*Figure 2-1 - Area selected in the North Sea (green area) where the AIS data was extracted for the year 2023.*

The dataset from the AIS consists of the journeys of vessels that have sailed in the selected area in 2023. The dataset provides a unique track identity (ID) for each track/journey of a ship. For each journey, the following information is provided: date and time, the maritime mobile service identity (MMSI) number, SOG, longitude, latitude, course over ground, heading, and actual draught. These parameters are recorded every minute. A dataset of the main particulars of the vessels sailing in the selected area is also available, which consists of the following information: track ID, MMSI, International Maritime Organization (IMO) number, length overall, breadth, AIS ship type, built year, gross tonnage, net tonnage, deadweight, Lloyd's ship type, scantling draught, among other parameters of less importance for this study. To obtain the vessel main particulars for each journey, the MMSI number was used to merge both datasets. The service speed and cavitation inception speed were not provided in the dataset. These speeds are estimated from empirical relations in Chapter 3.

## 2.2 Vessel categories

The vessels investigated in this study were classified in six categories: fast container, slow container, bulker, tanker/LPG (liquefied petroleum gas), LNG (liquefied natural gas) carrier, and vehicle carrier. Fishing, tug, naval, recreational, government, research, cruise, passenger, dredger, and other vessel classes were not considered in the current study. The six categories used in this study are defined to be consistent with the J-E model (MacGillivray and de Jong 2021) and the ECHO-RNL model (Hannay, et al. 2019) because this model will be used to estimate the sound levels emitted by the vessels sailing in the selected area of the North Sea in Chapter 4. However, some changes were made in relation to the classification used in the J-E model. An overview of the categories used in this study and in the J-E model and how they are defined are given in Table 2-1.

The first difference between the ship categories is that the information in the Lloyd's List Intelligence (LLI) is used in this study to classify the vessels instead of the AIS ship type ID (used in the J-E model). In the J-E model, the distinction between container and bulker is mainly due to the average sailing speed. Because of this and because the LLI is used in this study, one extra category was created, named "slow container", and the category called container in the J-E model, is here referred to as "fast container". This was possible because the LLI defines if the vessel is a container or bulker, which is not possible only from the AIS ship type ID. The distinction between a bulker and a slow container is important to estimate the service speed and the cavitation inception speed more accurately since these speeds are obtained from empirical formulations that are ship type dependent. Another point to be kept in mind is that the speed through water (STW) was used in the J-E model to determine if a vessel was a container or bulker. In this study, the SOG was used as the estimation of the STW using hindcast data of current, wind and waves was outside the scope of the present study. To avoid that a vessel would be classified, for example, as a fast/slow container for one journey and then as a bulker for another journey because of its average SOG, the classification of a vessel (a MMSI number) was made based on all journeys performed by the specific vessel (MMSI number) for the entire year.

Another difference is the creation of an extra category named LNG. The LNG carriers were included in a separate category from the tankers and LPG carriers because their service speed is usually significantly higher than for oil and gas tankers. Thus, by creating a separate category for the LNG carriers, a more accurate estimation of the service speed and cavitation inception speed can be obtained for these vessels. This will be further discussed in Section 3.1.

By comparing the AIS ship type ID for the ship categories in this study and the ones in the J-E model, we can see that the ID numbers are quite similar. The categories used in the current study include other AIS ship type ID than the ones defined by the J-E model, but these is a small part of the data, which should have a negligible effect on the results obtained for these categories.

Table 2-1 - Ships categories considered in this study.

Ship category	Current study		JOMOPANS-ECHO model	
	Definition from Lloyd's List Intelligence	AIS ship type ID (No. of unique vessels)	Ship class	Definition using AIS ship type ID
Fast container	Container/Bulker, $SOG > 16$ kn	70 (81), 90 (1)	Container	71-74 (all speeds) 70, 75-79 ( $V > 16$ kn)
Slow container	Container, $SOG \leq 16$ kn	0 (10), 33 (1), 70 (1877), 90 (14), 152 (2)	Bulker	70, 75-79 ( $V \leq 16$ kn)
Bulker	Bulker, $SOG \leq 16$ kn	0 (5), 33 (1), 35 (3), 52 (1), 70 (1214), 80 (1), 90 (7)	Bulker	70, 75-79 ( $V \leq 16$ kn)
Tanker/LPG	Tanker (oil/chemical) and LPG	0 (3), 70 (2), 80 (1066), 90 (5)	Tanker	80-89
LNG	LNG	80 (54)	Tanker	80-89
Vehicle carrier	Vehicle carrier	0 (2), 70 (339), 90 (7)	Vehicle carrier	n/a

### 2.3 Distribution of ships in the North Sea

The number of unique ships and the total number of journeys in the selected area of the North Sea in 2023 per ship category are shown in Figure 2-2. The majority of vessels sailing in this area are slow containers, which also perform the largest number of journeys in 2023. Following that, bulkers and tankers/LPG carriers are the second and third ship categories with the highest number of unique vessels sailing in the selected area. Vehicle carriers follow with 348 unique ships, and fast containers and LNG carriers represent a small portion of unique vessels. Regarding the number of journeys, slow containers perform the largest number of journeys, followed by tankers/LPG carriers and bulkers. Following that are the vehicle carriers, and the fast containers and LNG carriers comprise a small number of journeys.

Figure 2-2 also shows the number of unique vessels per number of journeys. On average, each vessel classified as a slow container performed around six journeys in 2023. Following that are fast containers, vehicle carriers, and tankers/LPG carriers, with an average of five journeys per vessel.

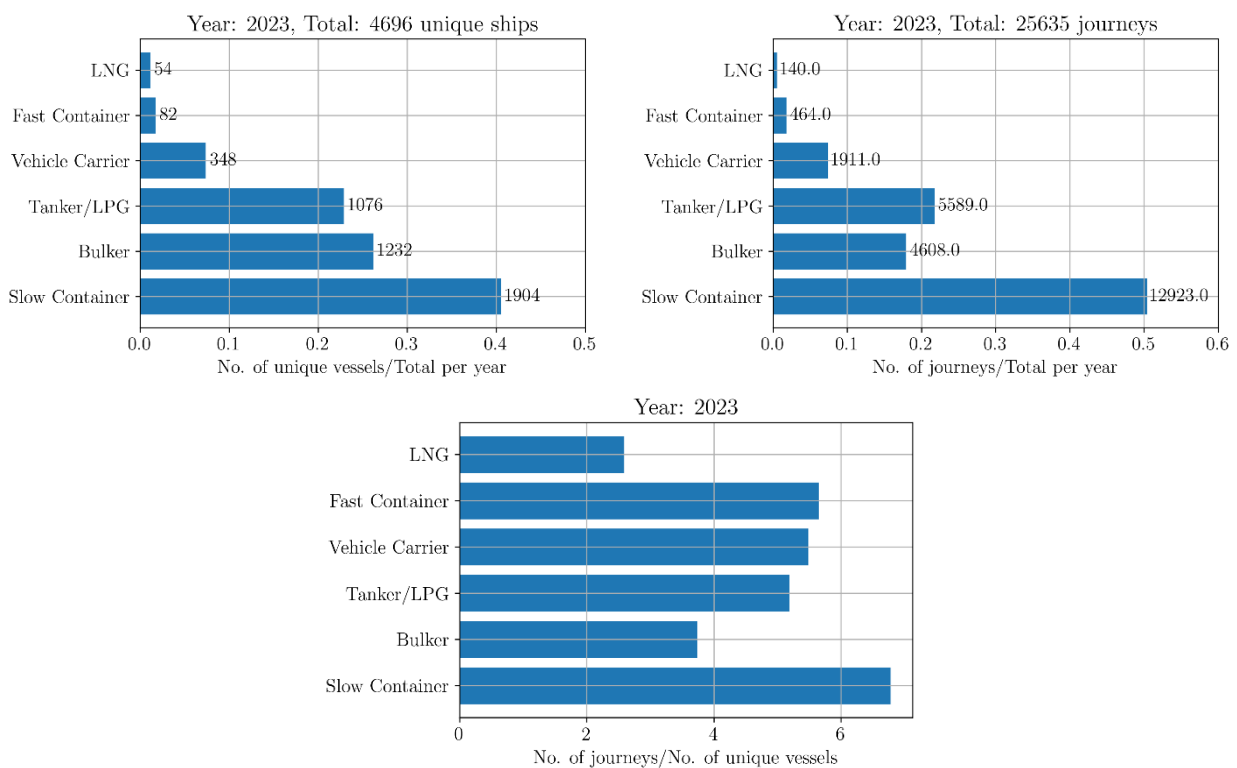


Figure 2-2 - Normalised number of unique vessels, normalised number of journeys and number of journeys per number of unique vessels for 2023 for the North Sea area selected.

### 2.4 Statistical distribution of speed over ground in the North Sea

To analyse the statistics of the SOG in the selected area in the North Sea, two filters were applied to the SOG. The first filter discarded any data point at which the speed was below or equal to 3 kn to avoid the influence of stationary or very slow-moving vessels in the statistics for each ship category. The second filter verified the variation of the SOG through time for each journey. If the standard deviation of the SOG was larger than 10% of the mean SOG for a journey, this journey was discarded. This filter has the aim to remove any journey where the vessel was decelerating/accelerating to a port or for other reasons.

To obtain the statistics of the SOG, the average SOG for each journey was computed and the probability distribution of these values determined. Figure 2-3 shows the probability density distribution, commonly referred to as PDF, of the average SOG per journey for the different ship types, including the mean and standard deviation and a Gaussian distribution. The cumulative density distribution, commonly referred

to as CDF, is included in the Appendix. The average value and its standard deviation for each ship category is also shown in Table 2-2. The fast container is the fastest ship type, with an average SOG of 17 kn. The slowest sailing vessel is the bulker, with an average SOG of 10.6 kn.

The PDF of the SOG follows a Gaussian distribution well for the bulker, fast container, tanker/LNG and LPG. This is more evident in the CDF in Figure A1-1. The PDF for the vehicle carrier is skewed towards lower SOG, whereas it is skewed towards higher speeds for the slow container. Even though the unique vessels within the slow container category have an average SOG below 16 kn, values for the SOG up to 20 kn are still observed for this vessel category.

In Figure 2-3, a vertical dashed line was included to indicate the speed limit according to the ECHO Program of voluntary vessel slowdown for each vessel category. Following the ECHO Program, the speed limit is 11 kn for bulkers and tankers/LPG, and 14.5 kn for containers and vehicle carrier. Here, it is considered that the LNG carriers also follow a speed limit of 14.5 kn. Based on these speed limits, the following percentage of journeys will be affected by the slowdown: approximately 41% for the bulker, 42% for the vehicle carrier, 85% for the fast container, 16% for the slow container, 67% for the tanker/LPG, and 45% for the LNG. Therefore, approximately 35% of the total number of journeys would be affected by applying the same speed limits as the ECHO Program. By considering that the slow containers would follow a stricter speed limit (11 kn instead of 14.5 kn) as they are considered a slow sailing vessel, 56% of its journeys would be affected by the slowdown. In this case, approximately 55% of the total number of journeys would be affected by the slowdown.

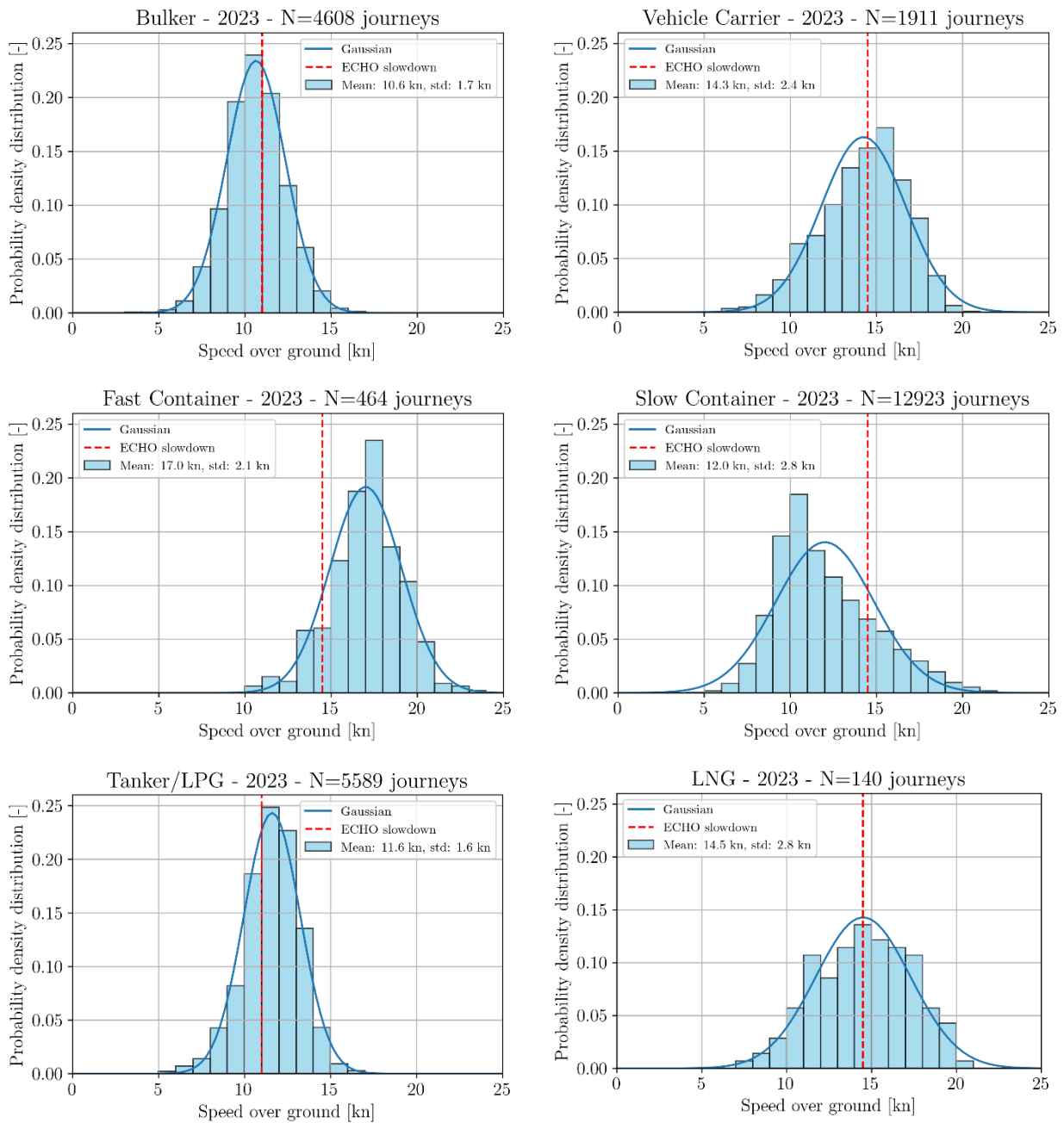


Figure 2-3 - Probability density distribution of the average speed over ground per journey for each ship type. Bin width of 2 kn. A Gaussian distribution based on the mean and standard deviation of the speed over ground is also included. The red-dashed line indicates the speed limit set in the ECHO Program of voluntary vessel slowdown.

Table 2-2 - Average SOG based on the average SOG per journey and the standard deviation for each ship type.

Ship category	Bulker	Vehicle carrier	Fast container	Slow container	Tanker/LPG	LNG
Average SOG [kn]	10.6	14.3	17.0	12.0	11.6	14.5
Standard deviation [kn]	1.7	2.4	2.1	2.8	1.6	2.8

### 3 STATISTICAL DISTRIBUTION OF THE CAVITATION INCEPTION SPEED AND SERVICE SPEED OF VESSELS SAILING IN THE NORTH SEA

In this section, the service speed and cavitation inception speed for the vessels sailing in the selected area in the North Sea are discussed. In Section 3.1, the estimation of the service speed is discussed and its distribution for the different ship types analysed. Afterwards, the determination of the cavitation inception speed is presented and its distribution for the different ship types discussed.

#### 3.1 Service speed

The service speed for the vessels sailing in the selected area in the North Sea was not available in the dataset. Thus, empirical formulations had to be used to estimate the service speed. De Jong and Hulskotte (2021) developed equations for the service speed as a function of the ship length overall ( $L_{oa}$ ) and the ship categories. They defined four categories, with Categories 1 and 2 of interest for this work. The service speed for these categories is given as:

$$V_s [kn] = \begin{cases} 17 + 7 \tanh\left(\frac{L_{oa}/1 [m] - 140}{50}\right), & \text{Category 1 (container, vehicle carrier, cruise)} \\ 12 + 3 \tanh\left(\frac{L_{oa}/1 [m] - 90}{25}\right), & \text{Category 2 (bulker, tanker)} \end{cases} \quad \text{Eq. 2}$$

where  $L_{oa}$  is in [m]. Based on the MAN reports for container ships (MAN Diesel 2008, MAN Energy Solutions 2024) for 2008 and 2023, it was observed that the service speed has decreased over the years, with a considerable decrease from 2014 onwards. Based on this, it was decided to develop new formulations for the service speed as a function of ship length for the container vessels, with different equations for ships build before and after 2014. These formulations followed the same format as the ones proposed by de Jong and Hulskotte, with new coefficients determined from fitting the equation to the data available in the MAN reports for 2008 and 2023. These new formulations are shown in Eq. 3.

A formulation was developed for the LNG carriers because they have higher service speeds compared to tankers for longer vessels. This new equation was based on the data available in the MAN report for LNG carrier of 2009 (MAN Diesel 2009) and followed the same format as the equations developed by de Jong and Hulskotte. This equation is shown in Eq. 3.

To verify the validity and define which equation should be used for each vessel category, comparisons of the service speed estimated from the equations by de Jong and Hulskotte and from the equations developed in this study are compared with the RINA Significant Ships database, where the service speed is known. These comparisons are shown in Figure 3-1.

The equation from de Jong and Hulskotte for the bulker shows a good agreement with the dataset. Thus, this equation is used to estimate the service speed for the bulker category. For the vehicle carrier, the new formulation for the container based on the MAN data for 2023 shows a better agreement with the dataset. Thus, this equation is used to estimate the service speed for the vehicle carriers. For the container ships, a good agreement is seen for the new formulations, showing that the distinction based on built year results in better estimates of the service speed. Hence, the new formulations based on the MAN reports are used to estimate the service for the fast and slow containers. The built year information was not available for all container ships in the AIS dataset used for this study. In these cases, the service speed was determined from the container ship equation given by de Jong and Hulskotte. For the tankers and LPG carriers, the equation by de Jong and Hulskotte for the tankers show a reasonable agreement with the Significant Ships dataset; thus, this equation is used in this study. For LNG carriers, we can clearly see that the new formulation based on the MAN report gives better estimates than the equation by de Jong and Hulskotte, mainly for ship lengths above 200 m.

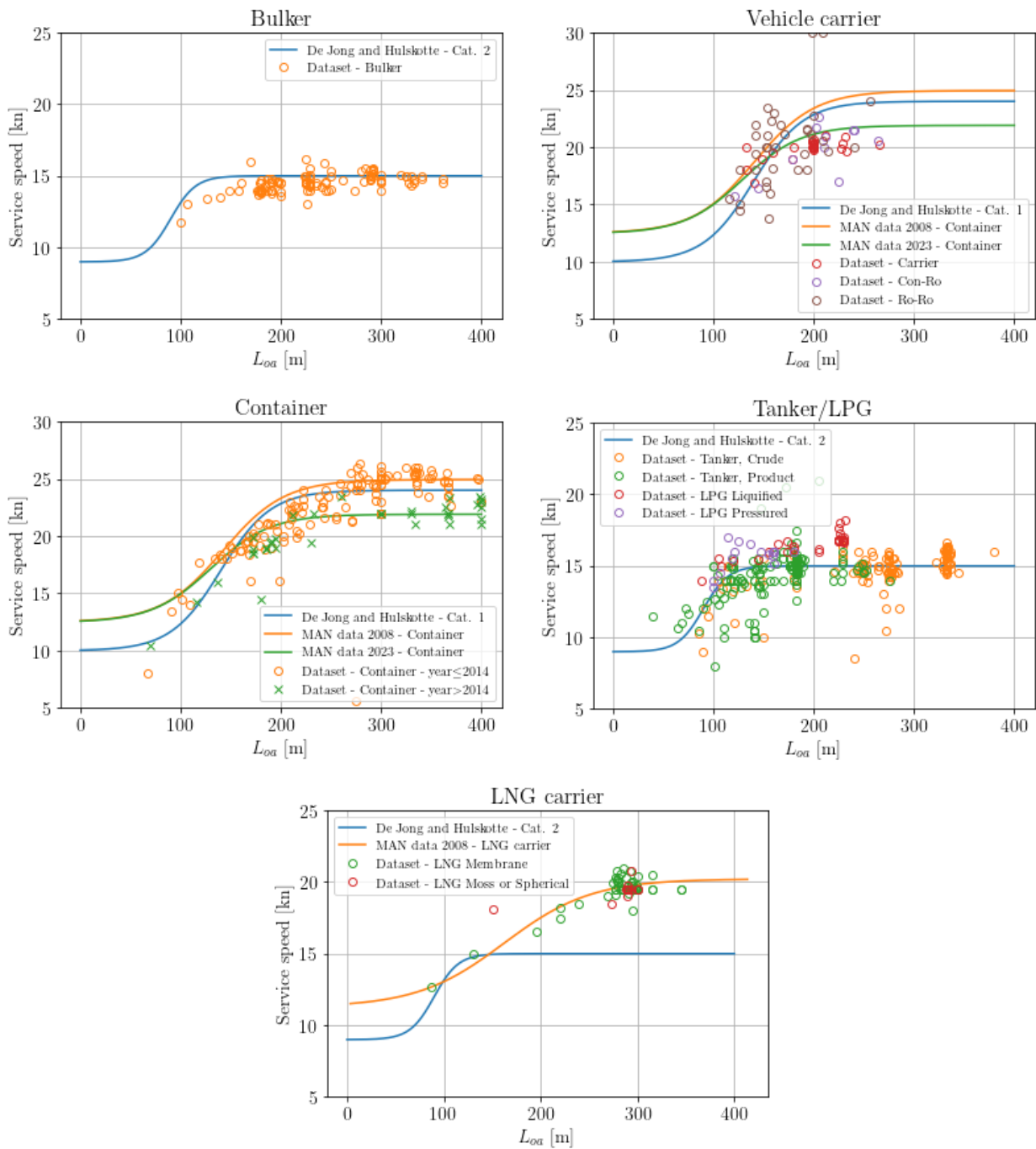


Figure 3-1 - Comparison of the service speed from the Significant Ships dataset and the formulations available to estimate the service for different ship categories.

Therefore, the formulations used in this study to estimate the service speed for the different vessel types are defined in Eq. 3 and represented in Figure 3-2.  $L_{pp}$  is the length between perpendiculars. Note that for some formulations, the length between perpendicular is used and for others the length overall. Only the length overall was available in the AIS data. Thus, the length between perpendicular was obtained based on the empirical formulations in (NAVISON 2023) and included in Eq. 4.

$$V_s [kn] = \begin{cases} 18.7 + 6.2 \tanh\left(\frac{L_{pp}/1 [m] - 151.7}{63.4}\right), & \text{Containers before 2014 (MAN data 2008)} \\ 17.2 + 4.7 \tanh\left(\frac{L_{pp}/1 [m] - 139.7}{61.0}\right), & \text{Containers after 2014 (MAN data 2023)} \\ & \text{and vehicle carriers} \\ 17.0 + 7.0 \tanh\left(\frac{L_{oa}/1 [m] - 140}{50}\right), & \text{Containers if year is not available} \\ & \text{(de Jong and Hulsotte)} \\ 15.7 + 4.5 \tanh\left(\frac{L_{pp}/1 [m] - 162.4}{89.8}\right), & \text{LNG carriers (MAN data 2009)} \\ 12.0 + 3.0 \tanh\left(\frac{L_{oa}/1 [m] - 90}{25}\right), & \text{Bulkers and tankers/LPG (de Jong and} \\ & \text{Hulsotte)} \end{cases} \quad \text{Eq. 3}$$

$$L_{pp} = -5.202 + 0.970 L_{oa}, \quad \text{for container vessels with } L_{oa} \text{ given in the AIS dataset}$$

$$L_{pp} = -4.637 + 0.958 L_{oa}, \quad \text{for vehicle carriers with } L_{oa} \text{ given in the AIS dataset}$$

$$L_{pp} = -3.302 + 0.975 L_{oa}, \quad \text{for gas carriers with } L_{oa} \text{ given in the AIS dataset}$$

Eq. 4

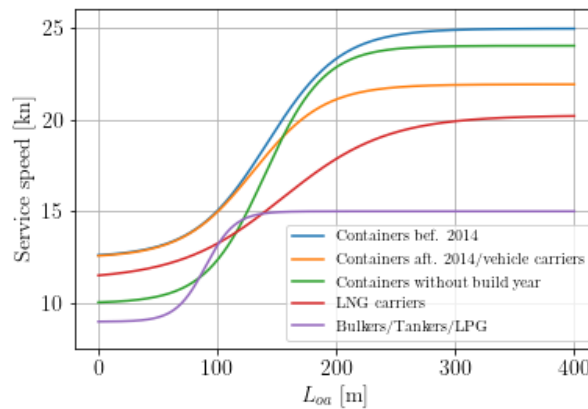


Figure 3-2 - Service speed as a function of the ship length overall.

Figure 3-3 shows the PDF of the average SOG normalised by the service speed for the journeys. The CDF is in the Appendix. For most journeys, the vessel operates below the service speed. For the fast container, some data is observed for SOG/service speed above 1.5. These cases are for vessels at which the build year was not available.



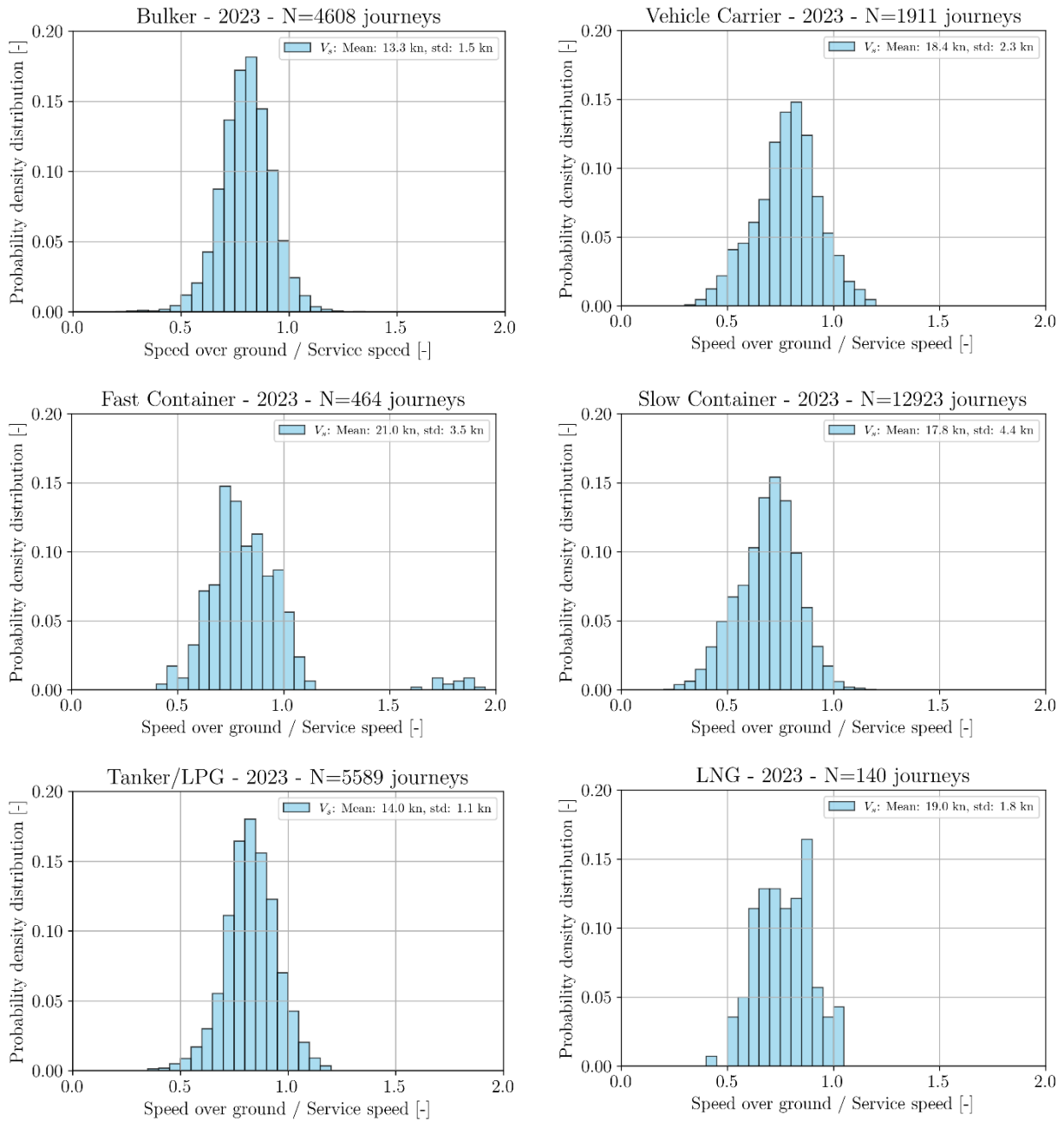


Figure 3-3 - Probability density distribution of the speed over ground normalised by the service speed per ship type. Bin width of 0.05.

### 3.2 Cavitation inception speed

The cavitation inception speed is estimated using a modified version of the formula proposed by (Jalkanen, et al. 2018):

$$V_{CIS}[kn] = \min \{ \max [ (1.42 - 1.2 C_B) \cdot V_S; V_{lower} ] ; 1.4 \}, \quad \text{Eq. 5}$$

where the additional variable  $V_{lower}$  has been introduced, being equal to 7 kn for bulker and tanker/LPG and 9 kn for all other ship types. The block coefficient,  $C_B$  can be estimated from the design Froude number, i.e., at the service speed,  $Fn_S$  (Watson 1995):

$$C_B = 0.7 + \frac{1}{8} \tan^{-1} \left( \frac{23 - 100 Fn_S}{4} \right), \quad \text{Eq. 6}$$

where  $Fn_s = V_s / \sqrt{gL_{wl}} \cong V_s / (3.13\sqrt{0.975L_{oa}})$  with the service speed in [m/s] and a fixed ratio between the waterline length ( $L_{wl}$ ) and the length overall has been assumed. The  $C_B$  values obtained from this equation is checked against the Significant Ships dataset for the different vessel types in Figure 3-4. The  $C_B$  in the dataset was not available for all vessels, but the block coefficient was computed for all ships in the dataset to verify if the estimated values are reasonable for each vessel category. As it can be seen from this figure, the block coefficient estimated from Eq. 6 in general shows a good agreement with the dataset values for the different categories. The average block coefficient for each vessel category is listed in Table 3-1.

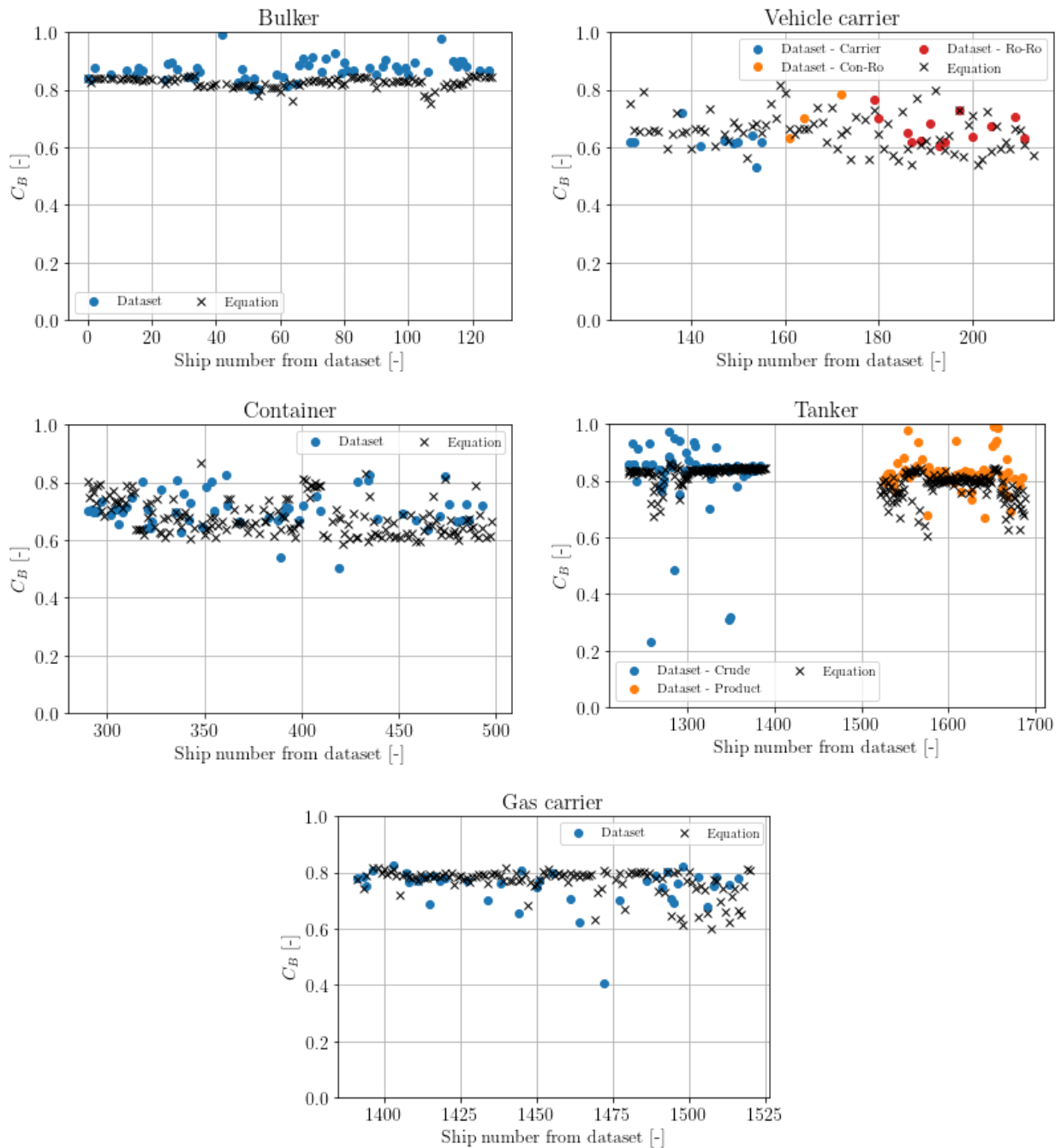


Figure 3-4 - Comparison of the block coefficient from the Significant Ships dataset with the formulation available to estimate the block coefficient (Eq. 6) for different ship categories. The x-axis show the ship number given to each vessel in the dataset.

Table 3-1 - Average block coefficient for each vessel category.

Ship category	Bulker	Vehicle carrier	Fast container	Slow container	Tanker/LPG	LNG
Average $C_B$	0.79	0.68	0.69	0.69	0.78	0.79

Figure 3-5 shows the PDF of the average SOG normalised by the cavitation inception speed for the journeys. The CDF is in the Appendix. A red-vertical line is included to indicate when the journey of a vessel is operating above the inception speed. For most journeys, the vessel operates above the inception speed: 98% of the journeys for bulkers, 87% of the journeys for vehicle carriers, 96% of the journeys for fast containers, 75% of the journeys for slow containers, 99% of the journeys for the tankers and LPG carriers, and 98% of the journeys for the LNG carriers. Therefore, for most journeys, the vessels are generating cavitation URN, which is an important contributor to the vessel total URN.

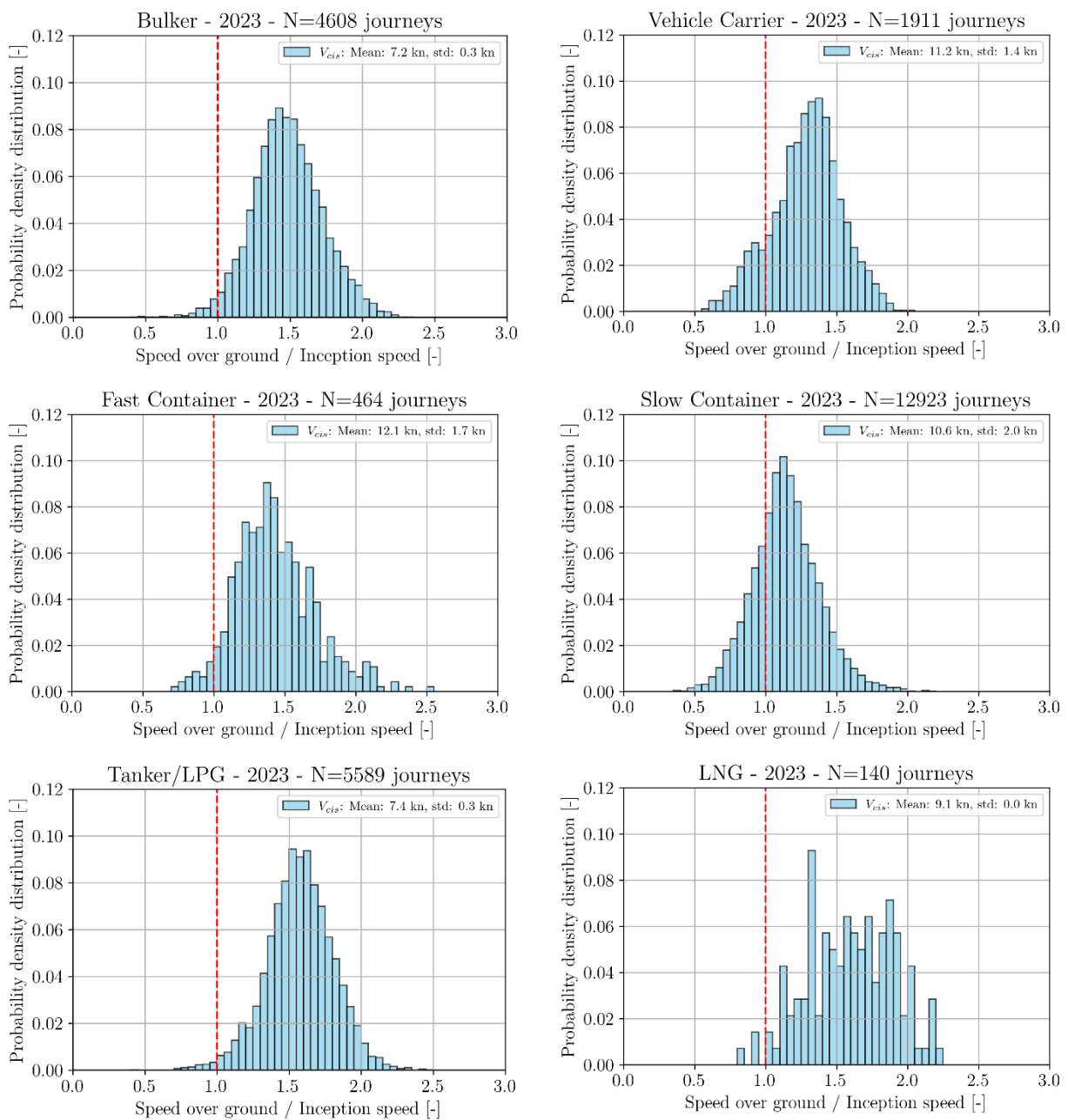


Figure 3-5 - Probability density distribution of the speed over ground normalised by the service speed per ship type. Bin width of 0.05.

## 4 SOUND LEVEL ESTIMATION FOR VESSELS SAILING IN THE NORTH SEA AND THE EFFECT OF SLOWDOWN

In this section, the sound levels for the different vessel categories sailing in the selected area in the North Sea are estimated from the J-E and the ECHO-RNL models. In Section 4.1, the models are described and a comparison between their radiated noise level estimates for the same cases analysed. The effect of applying the ECHO Program slowdown to the dataset investigated here is discussed in Section 0. The frequency range at which the noise estimated were performed are for decidecade frequency bands from 20 Hz to 20 kHz. The low-frequency range comprises frequencies from 20 Hz – 100 Hz, the mid-frequency range is for 100 Hz – 1 kHz, and the high frequency range is for 1 kHz – 20 kHz.

### 4.1 Prediction models for the radiated noise levels

The sound emitted by each ship category is estimated based on the radiated noise level (RNL) at each data point available for that ship category. Originally, the journey information in the AIS dataset was given every minute. This data was resampled to reduce the processing time of the data; for each journey, the available data, such as SOG, latitude, longitude, and actual draught, was averaged across 10-minute intervals. The RNL for each data point is then estimated using two models: the J-E source level (SL) model combined with a model to correct for Lloyd-mirror and the ECHO-RNL model. The main difference between these models is that the J-E model considers that the SLs scale with the ship speed to the power six for all frequencies and ship types, whereas the ECHO-RNL model considers the speed scaling as a function of frequency and ship type, resulting in a more accurate estimation of the URN levels with speed. Other more sophisticated models are also available (MacGillivray, Ainsworth, et al. 2022, Lloyd, et al. 2024), where the ship's draught, engine power, among other parameters, are also considered in the SL estimation. However, these models are not used in the current study because part of the required input parameters for these models are not available in the dataset used.

#### 4.1.1 J-E model

The J-E SL model consists of a baseline spectrum for each ship category and includes a speed scaling (to the power 6) and a length scaling (to the power 2). The baseline spectrum was developed based on the regression analysis for ship sound measurements performed within the ECHO Program. This model calculates the ship source spectral level, in decidecade frequency bands, as a function of frequency, speed, length, and AIS ship type. The model equations are given as:

$$L_{S,f}(f, V, L_{oa}, C) = L_{S,f,0}(f, C) + 10 \log_{10}(V/V_C)^6 \text{ [dB]} + 10 \log_{10}(L_{oa}/L_0)^2 \text{ [dB]} \quad \text{Eq. 7}$$

where  $f$  is the decidecade band centre frequency in [Hz],  $V$  is the ship speed in [kn], which is assumed to be equal to the SOG in this study,  $L_{oa}$  is the length overall,  $C$  is the ship class,  $V_C$  is a reference speed per vessel class, and  $L_0$  is a reference length equal to 91.44 m (300 ft). The baseline spectrum per ship type is given as:

$$L_{S,f,0}(\hat{f}, C) = K - 20 \log_{10}(\hat{f}_1) \text{ [dB]} - 10 \log_{10} \left( \left( 1 - \frac{\hat{f}}{\hat{f}_1} \right) + D^2 \right) \text{ [dB]} \quad \text{Eq. 8}$$

where  $\hat{f} = f/f_{\text{ref}}$ ,  $\hat{f}_1 = 480 \text{ Hz} \times (V_{\text{ref}}/V_C)$ ,  $f_{\text{ref}} = 1 \text{ Hz}$ ,  $V_{\text{ref}} = 1 \text{ kn}$ ,  $K = 191 \text{ dB}$ , and  $D = 3$  for all ship types, except  $D_{\text{cruise vessel}} = 4$ . For cargo vessels (container ships, vehicle carriers, bulkers, tankers), the J-E model includes an additional peak in the baseline spectrum below 100 Hz:

$$\begin{aligned}
 L_{Sf,0}(\hat{f} < 100, \text{Cargo}) &= K^{LF} - 40 \log_{10}(\hat{f}_1^{LF})[\text{dB}] + 10 \log_{10}(\hat{f}) [\text{dB}] \\
 &\quad - 10 \log_{10} \left( \left( 1 - \left( \frac{\hat{f}}{\hat{f}_1^{LF}} \right)^2 \right)^2 + (D^{LF})^2 \right) [\text{dB}]
 \end{aligned}
 \tag{Eq. 9}$$

with  $K^{LF} = 208 \text{ dB}$ ,  $\hat{f}_1^{LF} = 600 \text{ Hz} \times (V_{\text{ref}}/V_C)$ , and  $D^{LF} = 0.8$  for containers and bulkers or  $D^{LF} = 1.0$  for vehicle carriers and tankers.

The ship classes considered in the J-E model are: fishing, tug, naval, recreational, government/research, cruise, passenger, bulker, container ship, vehicle carrier, tanker, dredger, and other. These ship classes are defined based on the AIS ship type ID. However, the ship types in the current study are defined based on the LLI. As discussed in Section 2.2, this difference has a small influence in the classification. In this study, the interest is in the ship classes: bulker, container ship, vehicle carrier, and tanker. Thus, the reference speed  $V_C$  for these ship types is: 13.9 kn for the bulker, 18.0 for the container, 15.8 for the vehicle carrier, and 12.4 for the tanker.

In this study, two extra categories were defined in relation to the J-E model: slow container and LNG carrier. To be consistent with the model (see Table 2-1), the SL for the slow container is estimated based on the equations for a bulker and the levels for the LNG carrier is estimated from the equations for a tanker. The CDF of the SLs for each vessel type defined in this study are included in the Appendix.

The RNLs from the J-E SLs are obtained following the ISO 17208-2 (ISO 2019). According to this standard, the equivalent monopole SL can be obtained from the RNL by considering the propagation loss in a dipole source sound field in deep water. This yields a correction factor for the effect of the presence of the free surface on the acoustic field, usually referred as the Lloyd's mirror effect. The left image in Figure 4-1 illustrates the Lloyd's mirror effect, showing the direct and indirect paths of the sound wave between source and receiver. In this figure,  $r_d$  is the distance between the source and receiver,  $r_i$  is the distance between the image source and receiver,  $r$  is the intermediate path between the direct and indirect paths,  $\theta$  is the angle between the free surface and the intermediate path, and  $d$  is the source depth. The correction for an averaged grazing angle of  $15^\circ$ ,  $30^\circ$  and  $45^\circ$  is given as:

$$L_S = L_{RN} + \Delta L, \tag{Eq. 10}$$

$$\Delta L = -10 \log_{10} \left( \frac{2(kd)^4 + 14(kd)^2}{14 + 2(kd)^2 + (kd)^4} \right), \tag{Eq. 11}$$

where  $L_{RN}$  is the RNL in [dB re  $1 \mu\text{Pa}^2\text{m}^2$ ],  $\Delta L$  is the Lloyd's mirror correction in [dB],  $k = 2\pi/\lambda$  is the acoustic wavenumber in [1/m], with  $\lambda$  the acoustic wavelength in [m]. The right image in Figure 4-1 shows the Lloyd's mirror correction as a function of frequency. Therefore, the above equations can be used to estimate the RNLs from the SLs. In the development of the J-E model, a sophisticated propagation model was used to convert the RNL into SL, which has not been applied in the current study because it was outside of the scope. Hence, only a simplified correction (Lloyd's mirror correction) is applied to convert SL to RNL here.

According to the ISO 17208-2 (ISO 2019), the nominal source depth is defined as 70% of the vessel's actual draught. However, a nominal source depth of 50% was used when developing the J-E model; the ISO had not been released yet at the time of the publication. Therefore, to be consistent with the model, the nominal source depth was set to 50% of the actual draught, with the actual draught being given in the AIS data.

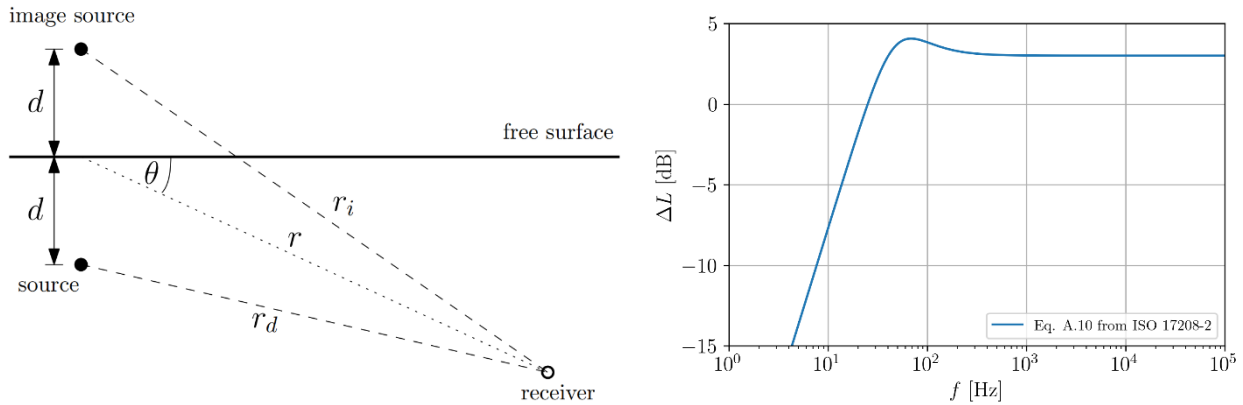


Figure 4-1 - Left: schematic of the Lloyd's mirror effect in the context of the ship sound measurement. Right: Lloyd's mirror correction as a function of  $f$  for  $d = 10$  m.

#### 4.1.2 ECHO-RNL model

The ECHO-RNL model was developed based on measurements performed within the ECHO Program and gives the RNL as a function of the decidecade frequency band and ship type and it scales the sound levels with the STW, which in the case of this model is frequency dependent. The ECHO-RNL model gives the spectral density as:

$$L_{RN}(f, C, V) = L_{RN,mean}(f, C) + 10 \log_{10}(V/V_C)^{STW_{coef}(f)} \quad \text{Eq. 12}$$

where  $C$  is the ship class,  $V$  is the ship speed in [m/s], which is assumed to be equal to the SOG in this study,  $L_{RN,mean}$  is the baseline RNL spectrum per ship class in [dB re  $1\mu\text{Pa}^2\text{m}^2$ ],  $STW_{coef}$  is the speed scaling coefficient, and  $V_C$  is the reference speed per ship type given in [m/s].  $V_C$  is 7.41 m/s for the bulker, 10.39 m/s for the container, 7.46 m/s for the tanker, and 9.41 m/s for the vehicle carrier.

Figure 4-2 shows the baseline spectrum and the STW coefficient as a function of decidecade frequency bands. The speed scaling (STW coefficient) differs considerably with the vessel type and frequency band. Tankers present the lowest speed scaling, reaching almost a zero scaling at 1 kHz. Vehicle carriers and containers have the highest speed scaling of approximately to the power 5 at low frequencies (below 100 Hz) and at around 10 kHz.

When analysing the effect of slowdown, it is expected that the J-E model results in more optimistic URN reductions because it considers a speed scaling to the power 6 (see Eq. 7) for all frequencies and vessel types, whereas a much lower scaling is in fact observed (Figure 4-2). Therefore, a more accurate analysis of the real effect of the slowdown is expected from the radiated noise level estimations based on the ECHO-RNL model.

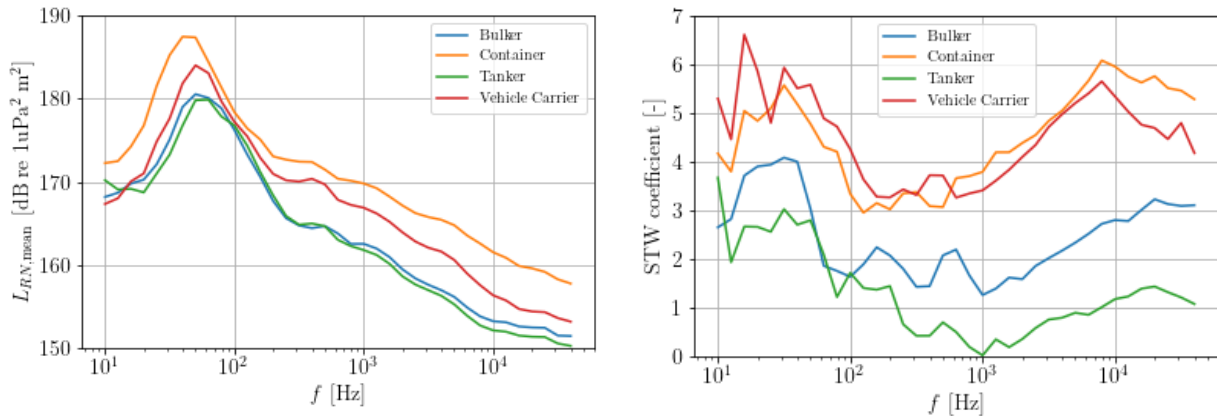


Figure 4-2 - Mean radiated noise level for different ship types and the speed scaling coefficient for the ECHO-RNL model.

In this study, two extra categories were defined in relation to the ECHO-RNL model: slow container and LNG carrier. As done for the J-E model, the noise levels for the slow container are estimated based on the equations for a bulker and the levels for the LNG carriers are estimated from the equations for a tanker.

The prediction of the RNL used in this study based on the ECHO-RNL model also considers the scaling of the ship length in the same manner as in the J-E model. Thus, the RNL from the ECHO-RNL model is determined as:

$$L_{RN}(f, C, V) = L_{RN,mean}(f, C) + 10 \log_{10}(V/V_C)^{STW_{coef}(f)} + 10 \log_{10}(L_{oa}/L_C)^2 \quad Eq. 13$$

where  $L_C$  is the reference length per ship type: 200 m for the bulker, 294 m for the container, 175 m for the tanker, and 199 m for the vehicle carrier.

#### 4.1.3 Comparison of the radiated noise level spectra for the J-E and ECHO-RNL models

Figure 4-3 shows the RNL spectra calculated for the J-E model and the ECHO-RNL model for the different ship types. For each ship type, three cases have been selected randomly from the dataset and the RNL was calculated for each case with both models. The main difference between the RNL estimated with the J-E model and the ECHO-RNL model is for low frequencies likely because no sound propagation model was used to compute the RNLs from the SLs for the J-E model. For frequencies above 200 Hz, a better agreement between the levels estimated by the models is observed. The RNL estimates for the slow container also show significant differences between the two models.

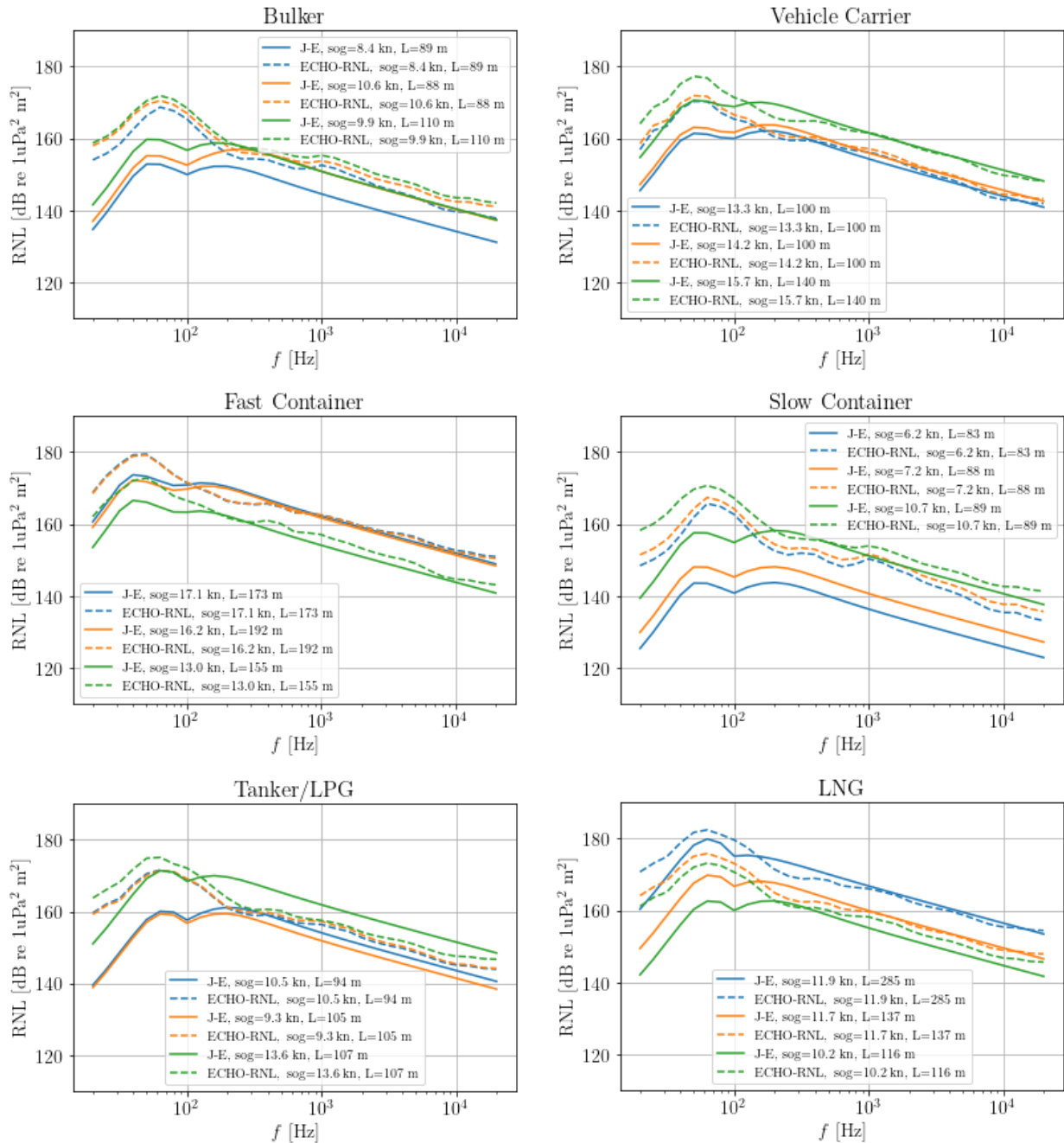


Figure 4-3 - Radiated noise levels estimated from the J-E model and the ECHO-RNL model for different ship categories. The RNL is estimated for three different conditions (speed over ground (sog) and length overall ( $L_{oa}$ )). These conditions were randomly selected from the dataset.



## 4.2 Slowdown analysis and effect

The effect of imposing a slowdown to the vessels sailing in the selected area in the North Sea are analysed in this section. The slowdown analysis is based on the Port of Vancouver 2023 ECHO Program of voluntary ship slowdown (Port of Vancouver 2024), where bulkers, tankers, ferries and government vessels were encouraged to sail at a maximum speed of 11 kn, and vehicle carriers, cruise ships and container vessels at a maximum of 14.5 kn.

To perform the slowdown analysis, the dataset for the North Sea was used as baseline. The slowdown was imposed in all vessels in this dataset as follows:

- Speed limit of 11 kn was imposed for the bulkers and tankers/LPG.
- Speed limit of 14.5 kn was imposed for the vehicle carriers, fast and slow container ships, and LNG carriers.

The slow container ships had a speed limit of 14.5 kn to be consistent with the ECHO Program because all containers had this speed limit. As the LNG carriers are in general fast sailing vessels, it was decided to set their speed limit at the highest value. The speed limit was set as the SOG because the STW was not available. Due to the slowdown, the journey time for the vessels had to be updated to take into account the delay caused by the lower sailing speeds.

Regarding the workflow of the analysis, the following sequence of steps was followed to investigate the slowdown effect on the noise levels:

1. Filters for the SOG to remove speeds below 3 kn and any considerably variation in the speed for a journey were applied.
2. The speed limit for the slowdown was imposed in the dataset based on the type of vessel and the journey times updated due to the delay because of the lower sailing speeds.
3. The data in time was resampled to 10-minute intervals.
4. The SL with the J-E model for each data point was computed and converted afterwards to RNL.
5. The RNL with the ECHO-RNL model for each data point was calculated.

In the next sections, two cases are analysed: the reference and the slowdown (SD). The workflow for the reference case is the same as the slowdown case, except that point (2) is not performed. At step 5, the RNL spectra was obtained for each data point.

### 4.2.1 Cumulative density distribution of the radiated noise level

Figure 4-4 shows the CDF of the RNL estimated with the J-E model and the ECHO-RNL model for the reference and the slowdown cases for each vessel category for a decidecade band of 125 Hz. The mean RNL for each model and each case is included in the figure legend. The CDF for a decidecade band of 63 Hz is included in the Appendix. The noise levels estimated based on the ECHO-RNL model present a smaller level spreading than the levels estimated from the J-E model because the J-E model has a stronger dependency on the speed (power 6 for the J-E model and power ranging from 1.4 to 3.6 for the ECHO-RNL model for a 125 Hz decidecade band).

Table 4-1 lists the level difference between the mean RNL for the slowdown and the reference cases for both models. The slowdown decreases the RNL in comparison to the reference case. According to the results for both models, the largest reductions are for the fast container and the vehicle carriers as these vessels sail at larger speeds (Table 2-2). In general, the mean RNL reduction based on the estimates from the J-E model are larger, as expected due to its stronger dependency on the ship speed. This is more critical for the bulkers, tankers/LPGs, LNG carriers and slow containers because the RNL for these vessels in reality scale to a much lower speed power than the power 6 for these frequency

bands (around 2; see Figure 4-2). The results for the decidecade band of 63 Hz from the J-E model should be regarded with caution because no propagation model was used to estimate the RNL from the SL, which has a more significant effect for lower frequencies.

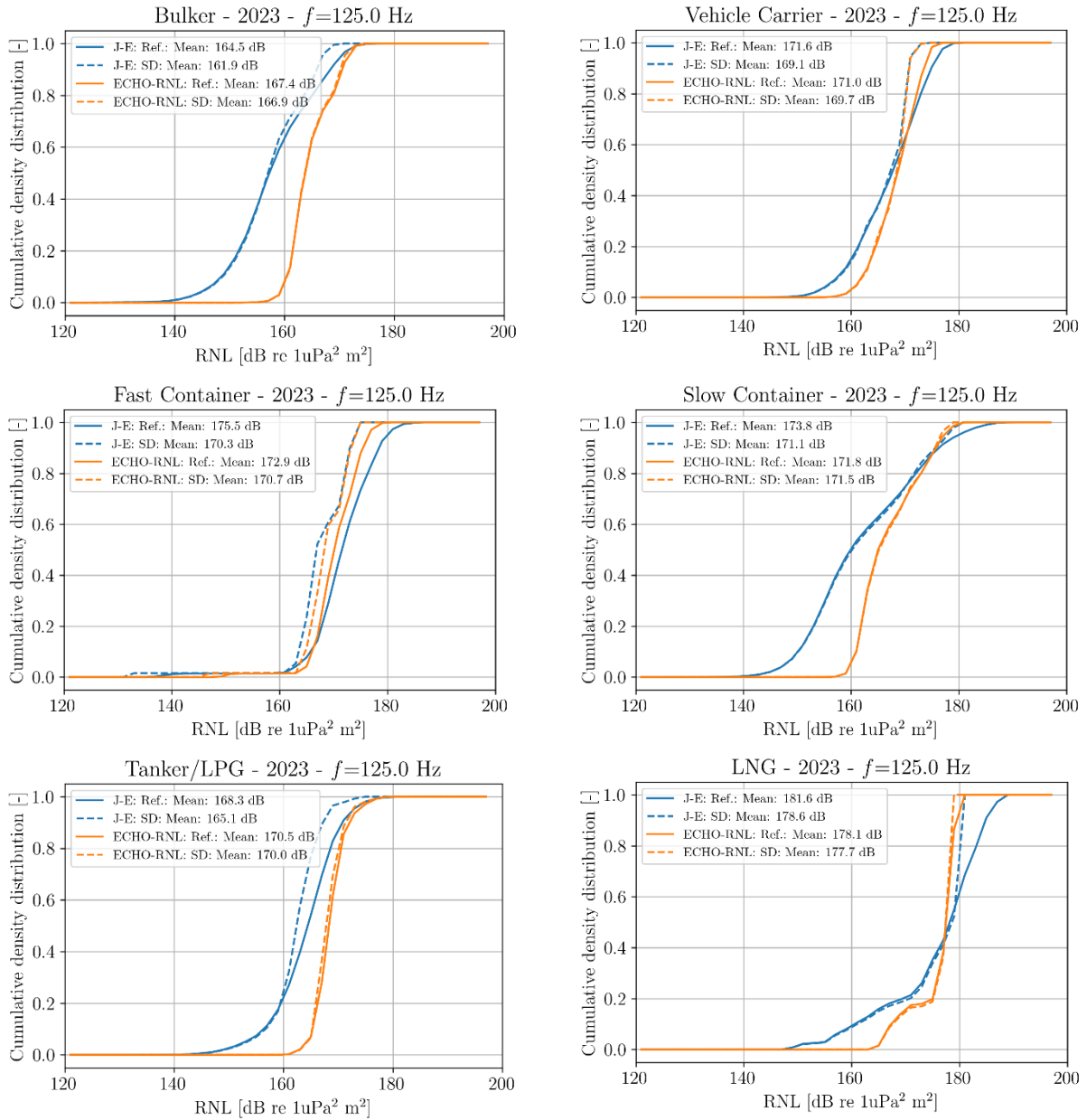


Figure 4-4 - Cumulative density distribution of the source levels for each ship category for a centre decidecade band of 125 Hz for two cases: reference and ECHO slowdown. The source levels are estimated based on the J-E model and the ECHO-RNL model. Bin width of 2 dB.

Table 4-1 - Difference of the mean RNL values between the slowdown and reference case for RNL estimates based on the J-E model and on the ECHO-RNL model for two decidecade frequency bands. Negative values indicate a reduction of the RNLs for the slowdown case.

Ship type	Mean RNL difference: slowdown – reference [dB]			
	J-E model	ECHO-RNL model	J-E model	ECHO-RNL model
	63 Hz	63 Hz	125 Hz	125 Hz
Bulker	-2.47	-0.47	-2.57	-0.48
Vehicle carrier	-2.61	-1.90	-2.57	-1.26
Fast container	-5.20	-3.46	-5.13	-2.24
Slow container	-2.80	-0.32	-2.68	-0.33
Tanker/LPG	-3.25	-0.84	-3.23	-0.53
LNG carrier	-2.95	-0.69	-2.98	-0.41

#### 4.2.2 Radiated noise exposure level

The sound exposure level is a measure that quantifies the sound over a specified time period that an animal would be exposed to. When a ship reduces its speed this exposure time will increase which should be considered as well. However, except for the Lloyd-mirror effect, the present study does not include sound propagation so it has been decided to use the radiated noise level as the relevant sound exposure metric. The sailing time of the ship in the selected area has been used as the exposure time period. No auditory weighting function has been included to account for a specific species in the RNLs. The resulting quantity is designated radiated noise exposure level (RNEL).

The total RNEL is calculated as the power summation of the RNL within a decidecade frequency band multiplied by the time interval that the vessel was emitting that RNL over all data points for a ship type during the year 2023:

$$RNEL(f) = 10 \log_{10} \left( \sum_{i=1}^N (10^{(L_{RN,i}(f)/10)}) \cdot \frac{\Delta t}{1 \text{ s}} \right) \text{ per ship type} \quad \text{Eq. 14}$$

where  $L_{RN}$  is in [dB re  $1 \mu\text{Pa}^2\text{m}^2$ ],  $N$  is the total number of data points for each ship category,  $\Delta t$  is the time interval at which the vessel was emitting the RNL for each data point in [s], and RNEL has units of [dB re  $1 \mu\text{Pa}^2\text{m}^2\text{s}$ ]. In general,  $\Delta t = 10 \text{ min}$  (600 s) due to the resampling of the data. This expression yields a spectrum for each vessel type thus corresponds with the total power of the sound emitted by each vessel category for the year of 2023. An annually average RNL per ship type can be obtained by dividing by the year period in seconds, resulting in:

$$RNL_{avg}(f) = 10 \log_{10} \left( \frac{\sum_{i=1}^N (10^{(L_{RN,i}(f)/10)}) \cdot \Delta t}{365 \cdot 24 \cdot 60 \cdot 60} \right) \text{ per ship type} \quad \text{Eq. 15}$$

with units of [dB re  $1 \mu\text{Pa}^2\text{m}^2$ ]. This quantity describes the level associated with the total power of the sound emitted by each vessel category for a time period of 1 s assuming that the vessel type is continuously present during the year. In this way the dependency of the RNEL on the time period is removed. It is stressed that this quantity is only introduced to predict a change in exposure level by shipping and that one has to be careful with the interpretation of the levels itself.

The results for this parameter are shown in Figure 4-5 for the J-E model and ECHO-RNL model for the reference and slowdown cases. The slow container has the highest RNL in the whole frequency range.

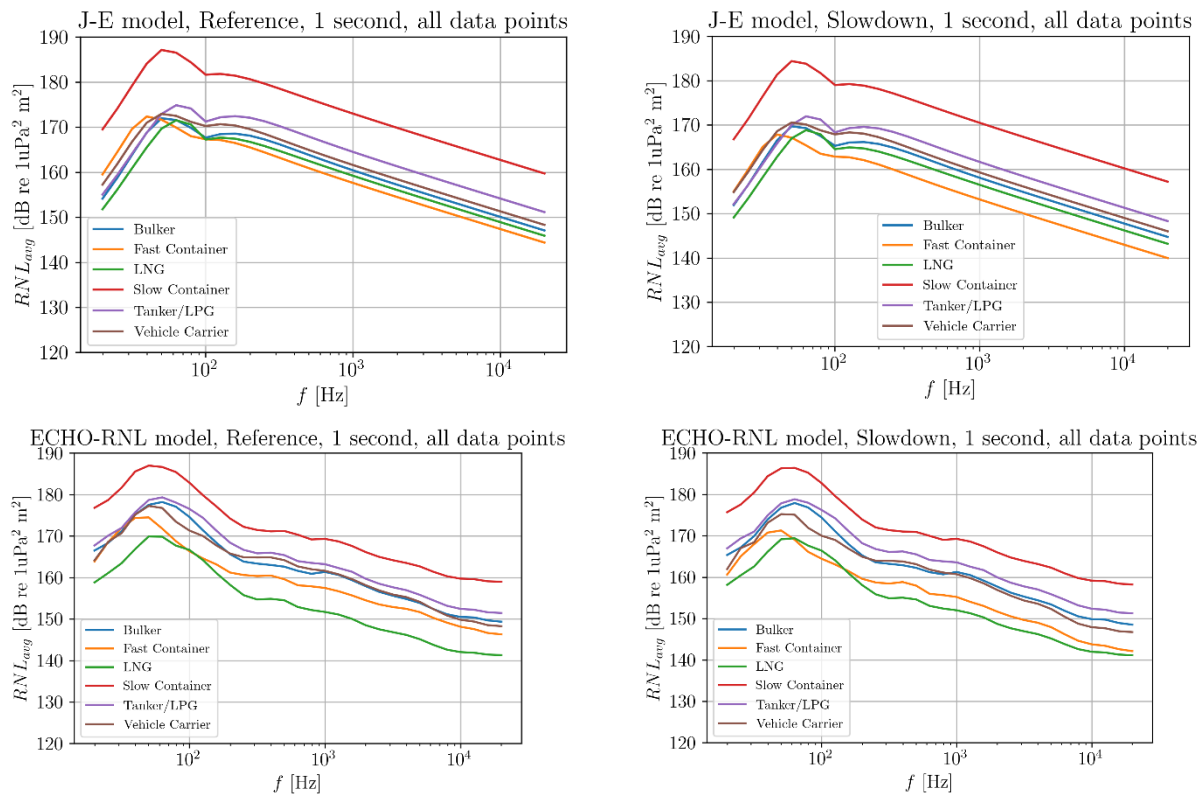


Figure 4-5 - Annually average RNL as a function of decidecade frequency bands for each ship category and for the reference and slowdown cases. The radiated noise levels were estimated based on the J-E model and the ECHO-RNL model. The levels correspond to  $RNL_{avg}$  considering all the data points.

The RNL difference between the slowdown case and the reference case has been computed for each noise estimation model and vessel type as a function of decidecade frequency bands. These results are shown in Figure 4-6. Note that the same difference in level between the slowdown and reference cases is obtained if  $RNL_{avg}$  is used instead of RNL. The RNL difference for the J-E model is roughly constant with frequency because this model considers a constant scaling of the speed with frequency. Based on this model, a reduction of the RNL is observed for all frequencies. The difference is around -2.3 dB for the bulkers, -4.4 dB for the fast containers, -2.7 dB for the LNG carriers, -2.6 dB for the slow containers, -2.9 dB for the tankers/LPG carriers, and -2.3 dB for the vehicle carriers.

For the ECHO-RNL model, smaller reductions in RNL are observed in comparison with the results for the J-E model, and the reductions vary with frequency. The tanker/LPG and LNG categories even show an increase in RNL around 1 kHz because the speed scaling for these vessels is near zero for these frequencies and these vessels have a longer journey time due to the slowdown, resulting in an increase of the RNL. The bulker, slow container, tanker/LPG and LNG categories result in RNL reductions of less than 1 dB in most frequencies, with an increase at around 1 kHz for the tankers/LPGs and LNGs. In contrast, the RNL reduction for these vessels according to the J-E model are between 2 and 3 dB. The fast containers are the most affected by the slowdown. It shows a reduction of a maximum of around 4 dB at low frequencies and 4.5 dB at high frequencies, which is the most similar to the results for the J-E model. However, in the mid-frequency range, a reduction of approximately 2 dB is expected, with the J-E model overestimating this reduction by more than 2 dB.

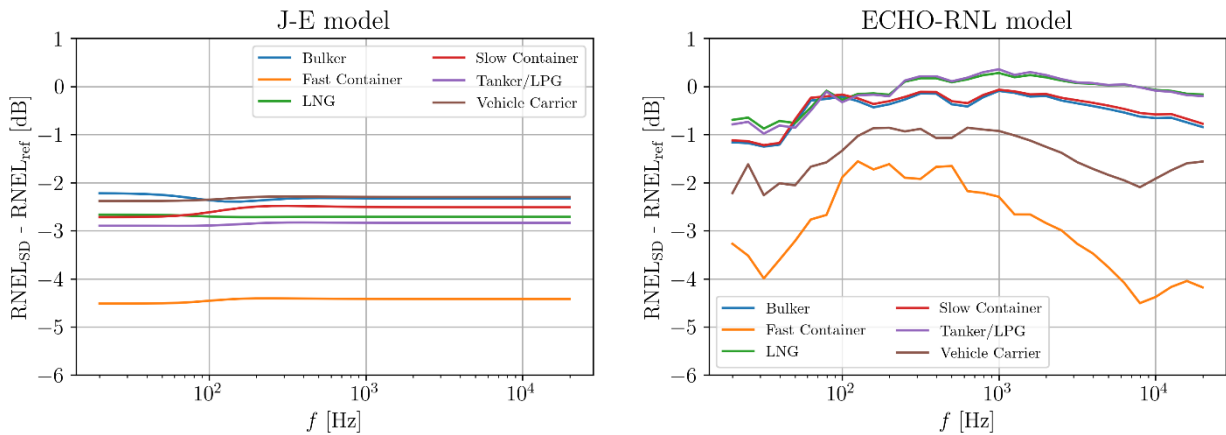


Figure 4-6 - Difference between the RNEL for the reference and slowdown cases. Negative values indicate a reduction of the RNEL when the slowdown is respected. The radiated noise levels were estimated based on the J-E model and the ECHO-RNL model.

Another metric computed to analyse the slowdown effect is the overall RNEL (ORNEL), which is calculated as the summation of the RNEL over decidecade frequency bands for each ship type:

$$ORNEL = 10 \log_{10} \left\{ \sum_{f=f_1}^{f_2} \left[ \sum_{i=1}^N (10^{(L_{RN}(f)/10)}) \cdot \frac{\Delta t}{1 \text{ s}} \right] \right\} \text{ per ship type} \quad \text{Eq. 16}$$

where  $f_1$  and  $f_2$  comprise the summation limit of the decidecade frequency bands of interest. Figure 4-7 shows the difference between the ORNEL for the slowdown and reference cases. Note that the same difference in level between the slowdown and reference cases is obtained if  $ORNL_{avg}$  (overall  $RNL_{avg}$ ) is used instead of ORNEL. The results for both models are shown and each figure shows the values for a different frequency range used to perform the summation of the RNEL. In general, the J-E model shows a larger reduction of the ORNEL. The largest differences are observed in the mid- and high-frequency ranges. In the high-frequency range, an increase of the RNEL is observed for the tanker/LPG and LNG categories. According to the ECHO-RNL results, the low-frequency range is the most affected by the slowdown for all vessel types. The ORNEL for the bulkers, tankers/LPGs, LNGs, and slow containers are not considerably affected by the slowdown due to their weaker dependency on the ship speed.

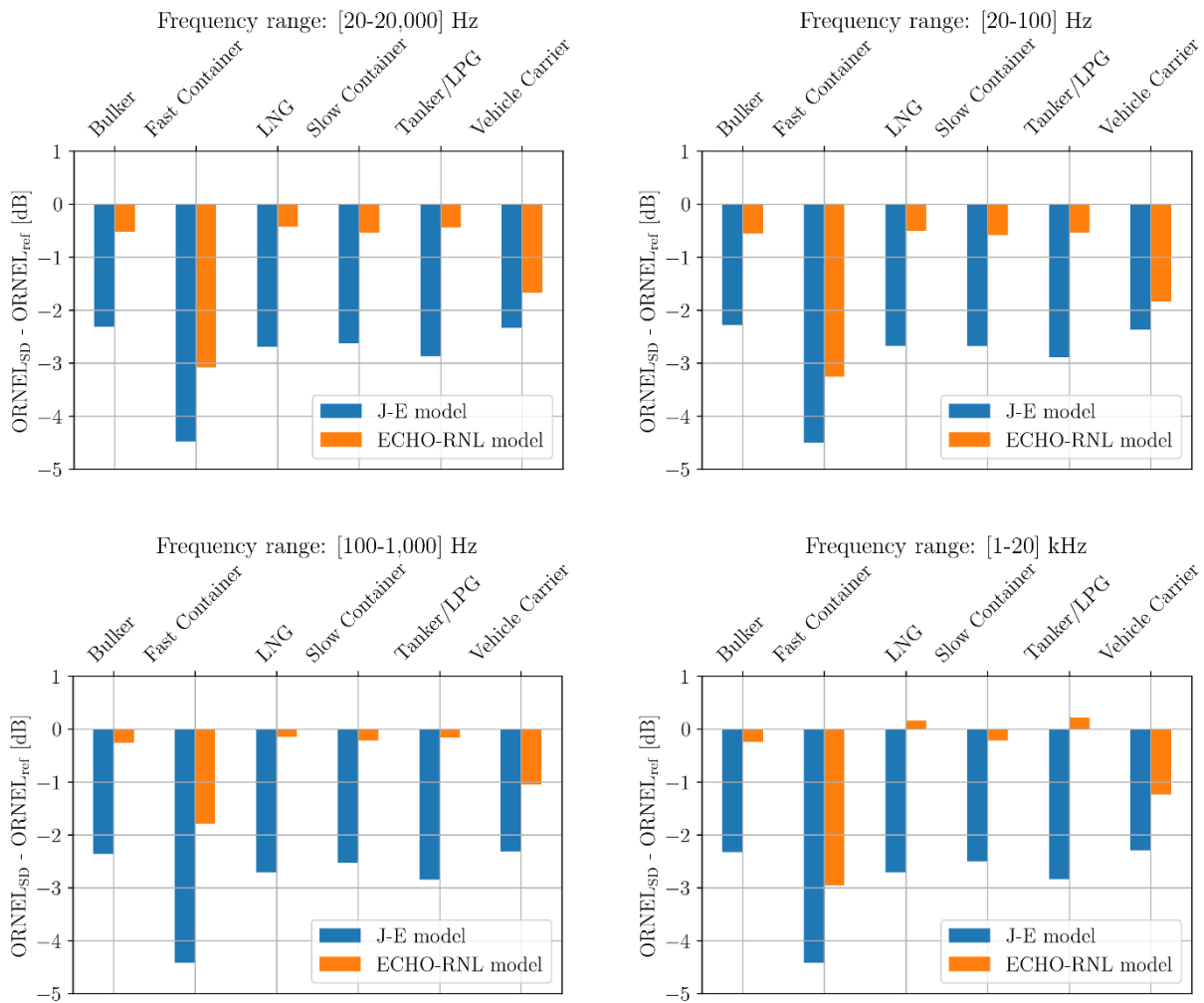
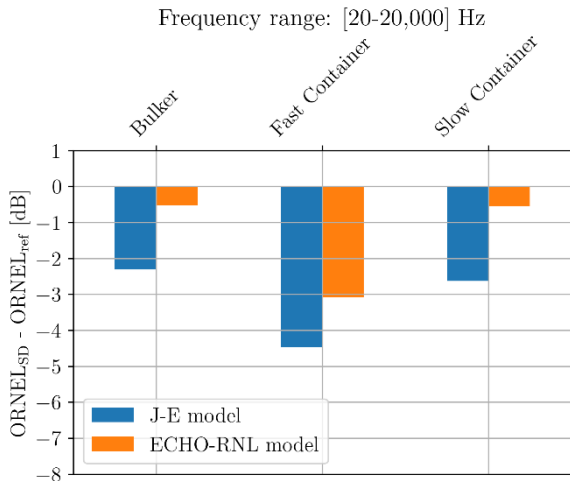


Figure 4-7 - Difference of the ORNEL between the slowdown (SD) and the reference (ref) cases for each ship type and source level model. The difference is shown for different frequency ranges considered to compute the ORNEL.

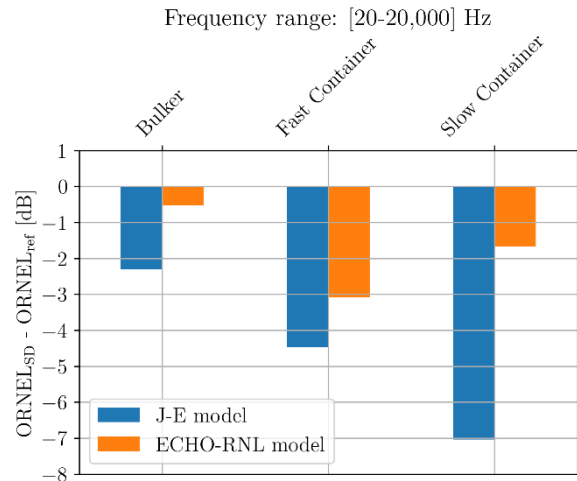
#### 4.2.3 Sensitivity of the results for the slow container vessels

An extra category of slow sailing container vessels was created in relation to the J-E and ECHO-RNL models, making a distinction between bulkers and containers for these vessels that sail at an average speed below 16 kn. Also, the ECHO slowdown measure did not discriminate between slow and fast sailing container vessels, so this category has been investigated in more detail with respect to its threshold speed used as selection criterion and the speed limit. Figure 4-8 shows the difference of the ORNEL between the slowdown (SD) and the reference (ref) cases for each ship type considering a different threshold speed to differentiate fast containers and bulkers/slow containers and a lower speed limit for the slowdown for the slow containers. The top left image is the same as Figure 4-7, and include here again as reference. By reducing the speed limit for slow containers from 14.5 kn to 11 kn, a larger reduction of the ORNEL is observed. This reduction is much more significant for the J-E model than for the ECHO-RNL model, as expected. For the J-E model, the ORNEL decreases to 7 dB for a speed limit of 11 kn, whereas it was less than 3 dB for a speed limit of 14.5 kn. For the ECHO-RNL model, the ORNEL decreases by only 1 dB in comparison to the speed limit of 14.5 kn.

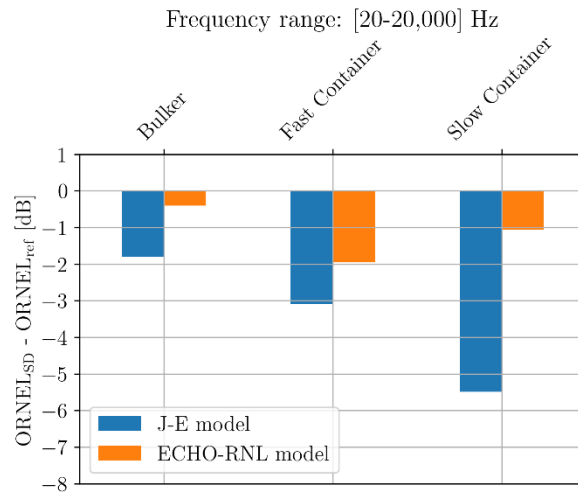
By considering a different speed threshold (13 kn instead of 16 kn), the ORNEL reduction due to the slowdown does not change significantly for the bulkers, but the estimated reduction for the fast and slow containers is affected. Thus, care must be taken when defining the bulkers and container ships.



a. Speed threshold: 16 kn; Speed limit for slow container: 14.5 kn



b. Speed threshold: 16 kn; Speed limit for slow container: 11 kn



c. Speed threshold: 13 kn; Speed limit for slow container: 11 kn

Figure 4-8 - Difference of the ORNEL between the slowdown (SD) and the reference (ref) cases for each ship type and noise estimation model. Each image shows the results for a different threshold speed to differentiate fast containers and bulkers/slow containers and for a speed limit for the slow containers.

#### 4.2.4 Journey time

Due to the slowdown implemented, the journey time for the vessels increase. Table 4-2 lists the average journey time with and without considering the slowdown based on the ECHO Program, the journey delay, and the average SOG without considering the slowdown. The fast containers suffer the largest journey delays due to their higher sailing speed, with an average delay of 29 min per journey. Next is the tanker/LPG vessels with an average delay of 18 min per journey, followed by the vehicle carriers with a 13 min delay and the bulkers with a 12 min delay. The slow containers have a very small average delay of 4 min per journey.

Table 4-2 - Average journey time with and without applying the slowdown, difference between the average journey times (journey delay), and average SOG without considering the slowdown.

Ship type	Average journey time without slowdown	Average journey time with slowdown	Delay using average journey times	Average speed over ground without slowdown [kn]
<b>Bulker</b>	4 h 49 min	5 h 01 min	12 min	10.6
<b>Fast container</b>	2 h 48 min	3 h 17 min	29 min	17.0
<b>LNG</b>	2 h 34 min	2 h 43 min	9 min	14.5
<b>Slow container</b>	4 h 22 min	4 h 26 min	4 min	12.0
<b>Tanker/LNG</b>	3 h 58 min	4 h 16 min	18 min	11.6
<b>Vehicle carrier</b>	3 h 40 min	3 h 53 min	13 min	14.3

The delay as a function of journey time without slowdown is also analysed in order to obtain extra insights into the delay times. The journey time without delay has been binned into 15-minute intervals and the average delay for each bin (i.e., each journey time) has been computed as well as the standard deviation of the delay and the number of journeys. Figure 4-9 show these results. In this figure, the normalised delay and number of journeys are also included. By analysing the mean delay, we observe two regions at which the delays are more significant: for journey times between 50 min – 300 min and between 500 min – 700 min. However, by analysing the normalised delay by the journey time, we observe that the most significant delays are observed for short duration journeys, below 200 min. Also, the number of journeys is small for journey times above 500 min. Note that these delays are only for the selected area of the North Sea. If the slowdown is implemented in the full journey or in a larger portion of the vessels journey, larger delay times would be obtained.



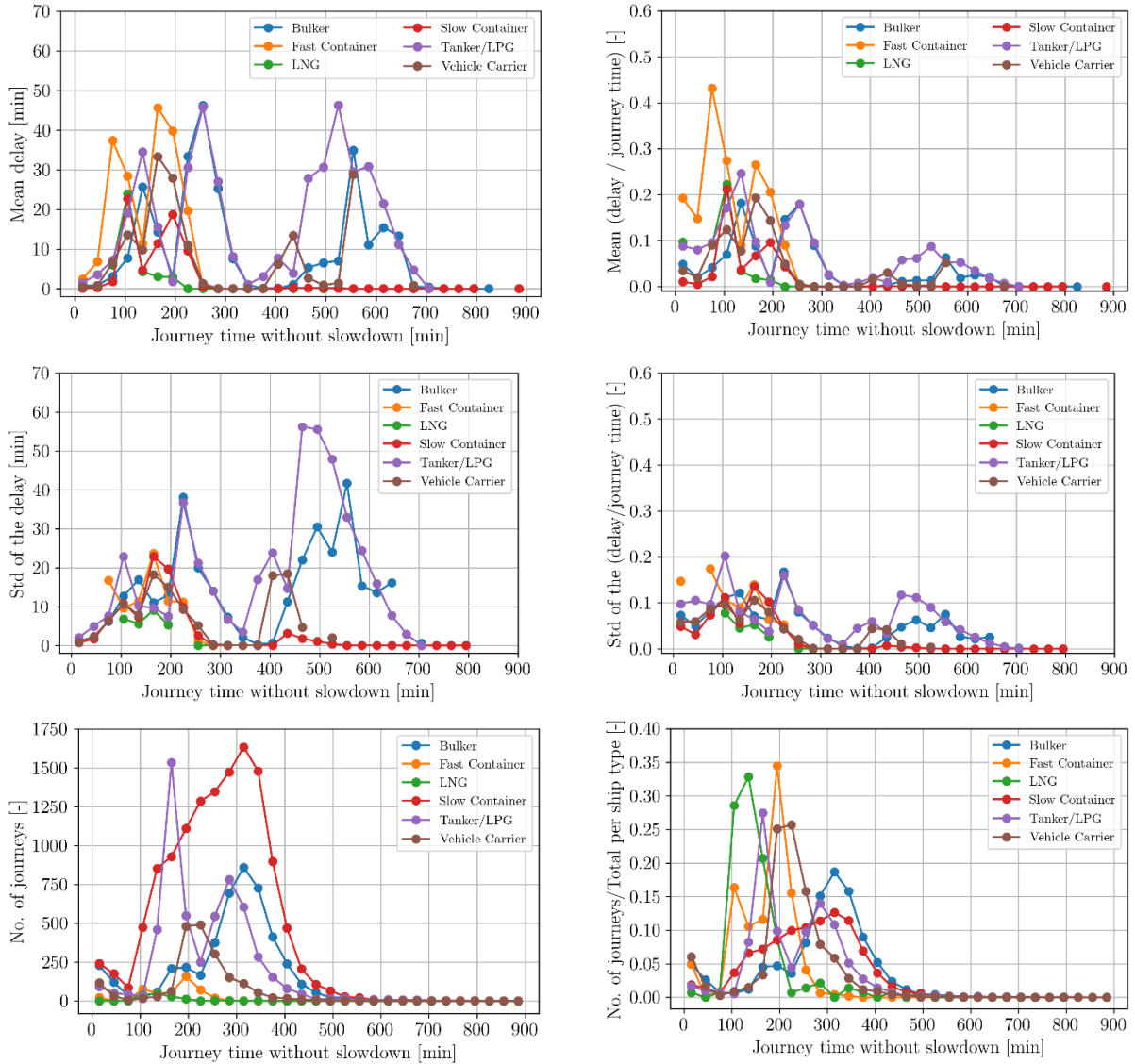


Figure 4-9 - Average journey delay, standard deviation of the journey delay and number of journeys as a function of the journey time without delay for the different ship categories. Absolute and normalised values are presented. The journey time without delay was binned in 15-minute intervals, with the centre value of each bin plotted in the graphs.

Figure 4-10 shows the CDF of the journey delay normalised by the journey time without slowdown for the different ship types. The normalised delay does not exceed 40% of the total journey time for most vessel types.

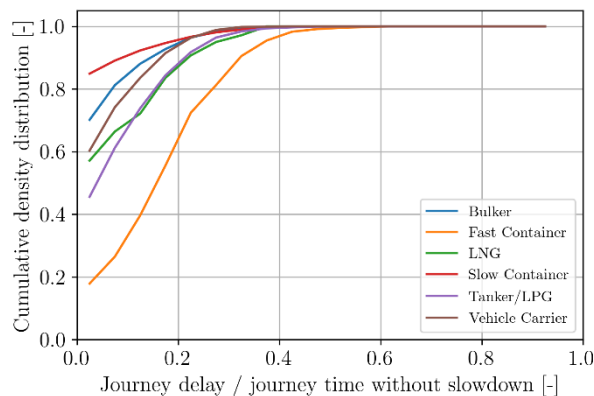


Figure 4-10 - Cumulative density distribution of the journey delay normalised by the journey time without slowdown for the different ship categories.

## 5 CONCLUSIONS

In the current study the effect of ship speed reduction on shipping noise in the Dutch part of the North Sea has been investigated for different types of vessels, using the speed limits as proposed by the ECHO slowdown program, which are: 11 kn for bulkers and tankers/LPGs, and 14.5 kn for vehicle carriers, container ships, and LNG carriers. Use has been made of AIS data for a selected part of the Dutch North Sea for the year 2023, combined with a ship database of Lloyds List Intelligence. A statistical analysis of the sailing speeds with respect to service speed and cavitation inception speed has been performed, with the main conclusions being:

- The majority of the ship journeys are performed by container ships sailing at a speed around 11 kn. For the URN models a distinction had to be made between slow and fast sailing container ships, for which a speed of 16 kn was used, but this distinction requires further attention.
- Approximately 35% of the ship journeys in the North Sea would be affected by the slowdown, but if a stricter speed limit is imposed to the slow sailing container ships (11 kn instead of 14.5 kn), this number increases to 55%.
- The large majority of the ships sailing in the North Sea (87% of the total journeys) operate at speeds higher than the estimated inception speed, indicating that cavitation noise is an important contributor to the underwater radiated noise in this region. However, the results for the cavitation inception speed must be regarded carefully because limited knowledge is available of the actual inception speed of individual merchant vessels.

The impact of slowdown on the sound level emitted by the vessels sailing in the Dutch North Sea is evaluated by criteria based on radiated noise levels (RNL). The effect of increased traveling time due to slowdown has been included by introducing the Radiated Noise Exposure Level (RNEL), which is the power summation of the RNL within a decidecade frequency band multiplied by the time interval that the vessel was emitting that RNL over all data points for a ship type during the year 2023. The Overall RNEL (ORNEL) is determined as the summation of the RNEL over decidecade frequency bands for each ship type. The RNL has been computed by two different empirical prediction methods: The Jomopans-Echo model is widely used but it uses a constant value for the ship speed dependency while the Echo-RNL model uses a ship speed dependency that is ship type and frequency dependent. The conclusions for this part are:

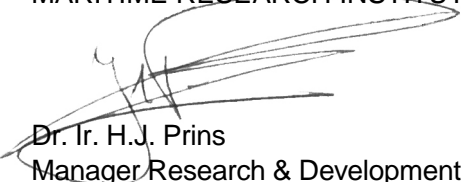
- In general, the slowdown results in lower sound levels for all vessel types.
- The reduction of the RNLs due to slowdown estimated with the J-E model are larger than the ones estimated with the ECHO-RNL model because the latter takes into account the speed dependency with frequency for each vessel type: maximum ORNEL reduction of 4.5 dB for the J-E model and 3 dB for the ECHO-RNL model.
- The largest differences between the two models for the ORNEL reduction are observed in the mid- and high-frequency ranges.
- According to the ECHO-RNL results, the low-frequency range is the most affected by the slowdown for all vessel types.
- The slowdown is more effective for fast-sailing ships (fast containers and vehicle carriers), with the fastest ship type (fast container) presenting a maximum speed reduction of 9.0 kn with an average reduction of 2.9 kn. A reduction in ORNEL of 3 dB and 1.7 dB are observed for the fast containers and vehicle carrier, respectively.
- For slow-sailing ships (bulkers, tankers/LPGs and slow-sailing containers), the slowdown results in a reduction of ORNEL but this reduction is smaller than for the fast sailing ships due to the weaker dependency of the RNL on the ship speed and a lower reduction of the sailing speed (maximum speed reduction of 6.5 kn with an average reduction of 1.3 kn for the slowest ship type – bulker). This results in an ORNEL reduction of less than 1 dB, increasing to 2 dB when a speed limit of

11 kn is applied to the slow-sailing containers. For the slow-sailing ships, it is expected that the contribution of machinery noise, that has a lower speed dependency than cavitation noise, is more relevant.

Based on the results of this study, recommendations of further investigations and developments are as follows:

- The striking differences of the estimated noise reductions for the J-E model and the ECHO-RNL model show the importance of considering the speed scaling in more detail and the complexity of trying to harmonise the different speed dependencies of machinery noise and cavitation noise in a single model. More advanced models, such as the one given in (Lloyd, et al. 2024) use a separate model for machinery noise and cavitation noise, but this model requires a substantial amount of additional information not available within the present project. Further statistical information on the contributions of machinery noise and cavitation noise and the cavitation inception speed within ship types is required to make more accurate predictions.
- Because the present study only considers RNL based criteria, it is also recommended to apply the results in a noise propagation model which allows the prediction of the actual change in ambient noise in the North Sea due to vessel slowdown.
- The ship category with the largest number of journeys is the container vessels, which was divided into slow sailing and fast sailing container ships. This subdivision was required because a similar procedure was adopted by the empirical noise prediction methods. However, as far as known, the ECHO slowdown study used the same speed limit for all container vessels. The threshold speed for slow/fast ships and the speed limit for slow container vessels has been briefly investigated in the present report showing the sensitivity of the results to these values. This aspect also requires further investigation as a further gain in reduction of radiated noise levels can be obtained by adjusting these speeds.

Wageningen, March 2025  
MARITIME RESEARCH INSTITUTE NETHERLANDS



Dr. Ir. H.J. Prins  
Manager Research & Development

**BIBLIOGRAPHY**

- Ainslie, Michael A. 2010. *Principles of sonar performance modeling*. Berlin: Springer.
- Arveson, Paul T., and David J. Vendittis. 2000. "Radiated noise characteristics of a modern cargo ship." *J. Acoust. Soc. Am.* 107: 118-129. doi:10.1121/1.428344.
- de Jong, C., and J. Hulskotte. 2021. *Reduction of ship traffic emissions and underwater noise - Part 2*. TNO report R10560, The Hague, the Netherlands: TNO.
- Duarte, Carlos M., Lucille Chapuis, Shaun P. Collin, Daniel P. Costa, Reny P. Devassy, Victor M. Eguiluz, Christine Erbe, et al. 2021. "The soundscape of the Anthropocene ocean." *Science* eaba4658.
- Erbe, Christine, Sarah A. Marley, Renée P. Schoeman, Joshua N. Smith, Leah E. Trigg, and Clare Beth Embling. 2019. "The Effects of Ship Noise on Marine Mammals—A Review." *Frontiers in Marine Science*.
- Findlay, C.R., L. Rojane-Donate, J. Tougaard, M.P. Johnson, and P.T. and Madsen. 2023. "Small reduction in cargo vessel speed substantially reduce noise impacts to marine mammals." *Science Advances*.
- Hannay, D.E., A.O. MacGillivray, H. Frouin-Mouy, Z. Li, F. Pace, J.L. Wladichuk, and Z. Alavizadeh. 2019. *Study of Quiet-Ship Certifications: Analysis using the ECHO Ship Noise Database*. Document Number 01737, JASCO.
- ISO. 2019. *ISO 17208-2 Underwater acoustics - Quantities and procedures for description and measurement of underwater sound from ships*. Geneva, Switzerland.
- Jalkanen, Jukka-Pekka, Lasse Johansson, Mattias Liefvendahl, Rickard Benschow, Peter Sigra, Martin Östberg, Ilkka Karasalo, Mathias Andersson, Heikki Peltonen, and Jukka Pajala. 2018. "Modelling of ships as a source of underwater noise." *Ocean Science* 1373-1383.
- Lloyd, T., Daniel J., Bosschers J., and M. Schuster. 2024. "PIANO: a physics-based semi-empirical source model for fleet-scale ship URN prediction." *Eight International Symposium on Marine Propulsors*. Berlin, Germany.
- Lloyd, Thomas, Evert-Jan Foeth, Frans Hendrik Lafeber, Johan Bosschers, Miloš Birvalski Yvette Klinkenberg, Levent Kaydihan, Artur Lidtke, and Erik van Wijngaarden. 2024. *Mitigation of ship underwater radiated sound by propeller optimisation and bubble injection*. Technical report Saturn D4.3, Wageningen: Maritime Research Institute Netherlands.
- Lucke, Klaus, Alexander O. MacGillivray, Michele B. Halvorsen, Michael A. Ainslie, David G. Zeddies, and Joseph A. Sisneros. 2024. "Recommendations on bioacoustical metrics relevant for regulating exposure to anthropogenic underwater sound." *JASA* 2508-2526. doi:10.1121/10.0028586.
- MacGillivray, A., and C. de Jong. 2021. "A reference spectrum model for estimating source levels of marine shipping based on automated identification system data." *Journal of Marine Science and Engineering*.
- MacGillivray, Alexander O., Laurie M. Ainsworth, Joanna Zhao, Joshua N. Dolman, David E. Hannay, Héloïse Frouin-Mouy, Krista B. Trounce, and Derek A. White. 2022. "A functional regression analysis of vessel source level measurements from the Enhancing Cetacean Habitat and Observation (ECHO) database." *J. Acoust. Soc. Am.*
- MacGillivray, Alexander O., Zizheng Li, David E. Hannay, Krista B. Trounce, and Orla M. Robinson. 2019. "Slowing deep-sea commercial vessels reduces underwater radiated noise." *JASA* 340-351.
- MAN Diesel. 2008. *Propulsion trends in container vessels*. Copenhagen, Denmark: MAN Diesel.
- MAN Diesel. 2009. *Propulsion trends in LNG carriers*. Copenhagen, Denmark: MAN Diesel.
- MAN Energy Solutions. 2024. *Propulsion trends in container vessels*. Copenhagen, Denmark: MAN Energy Solutions.
- NAVISON. 2024. *Calculation and analysis of shipping sound maps for all European seas from 2016 to 2050*. EMSA report, EMSA.
- NAVISON. 2023. *Integrated Vessel URN Soundscape Model*. Lisbon, Portugal: EMSA.
- Nelissen, Dagmar, Julius Kiraly, and Christiaan Meijer. 2022. *Blue Speeds for shipping - Economic analysis and legal framework to achieve environmental benefits*. Report, Delft: CE Delft.

- Port of Vancouver. 2024. *2023 Annual report - Enhancing Cetacean Habitat and Observation (ECHO) Program*. Annual report, Vancouver, Canada: Port of Vancouver.
- Southall, Brandon L., James J. Finneran, Colleen Reichmuth, Paul E. Nachtigall, Darlene R. Ketten, Ann E. Bowles, William T. Ellison, Douglas P. Nowacek, and Peter L. Tyack. 2019. "Marine Mammal Noise Exposure Criteria: Updated Scientific Recommendations for Residual Hearing Effects." *Aquatic Mammals* 125-232.
- Watson, D.G.M. 1995. *Practical ship design*. Oxford, UK: Elsevier.

# APPENDIX

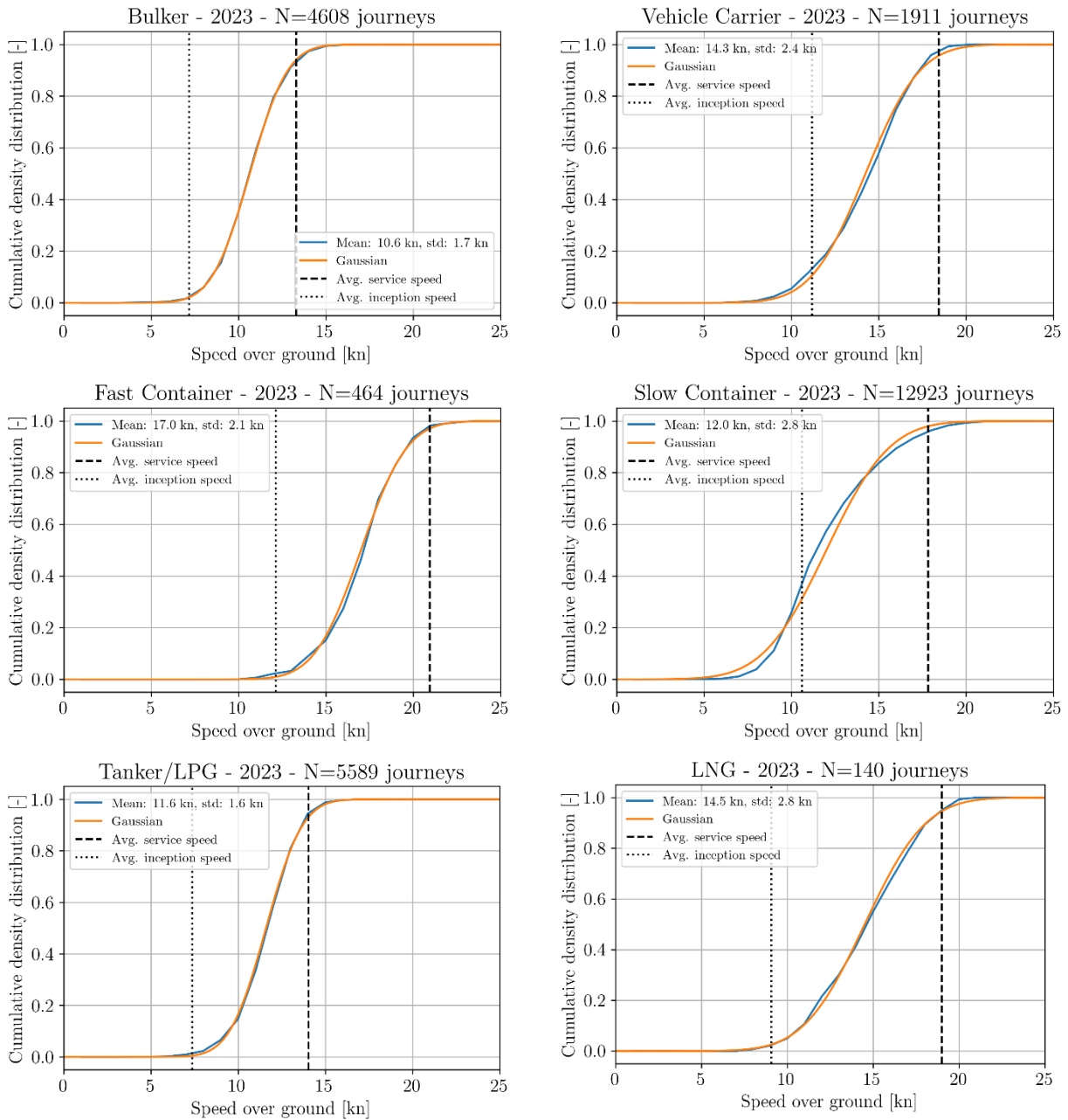
**APPENDIX 1**


Figure A1-1 - Cumulative density distribution of the speed over ground per ship type. Bin width of 2 kn. A Gaussian distribution based on the mean and standard deviation of the speed over ground is also included. The vertical lines indicate the average service speed and inception speed for each vessel type.

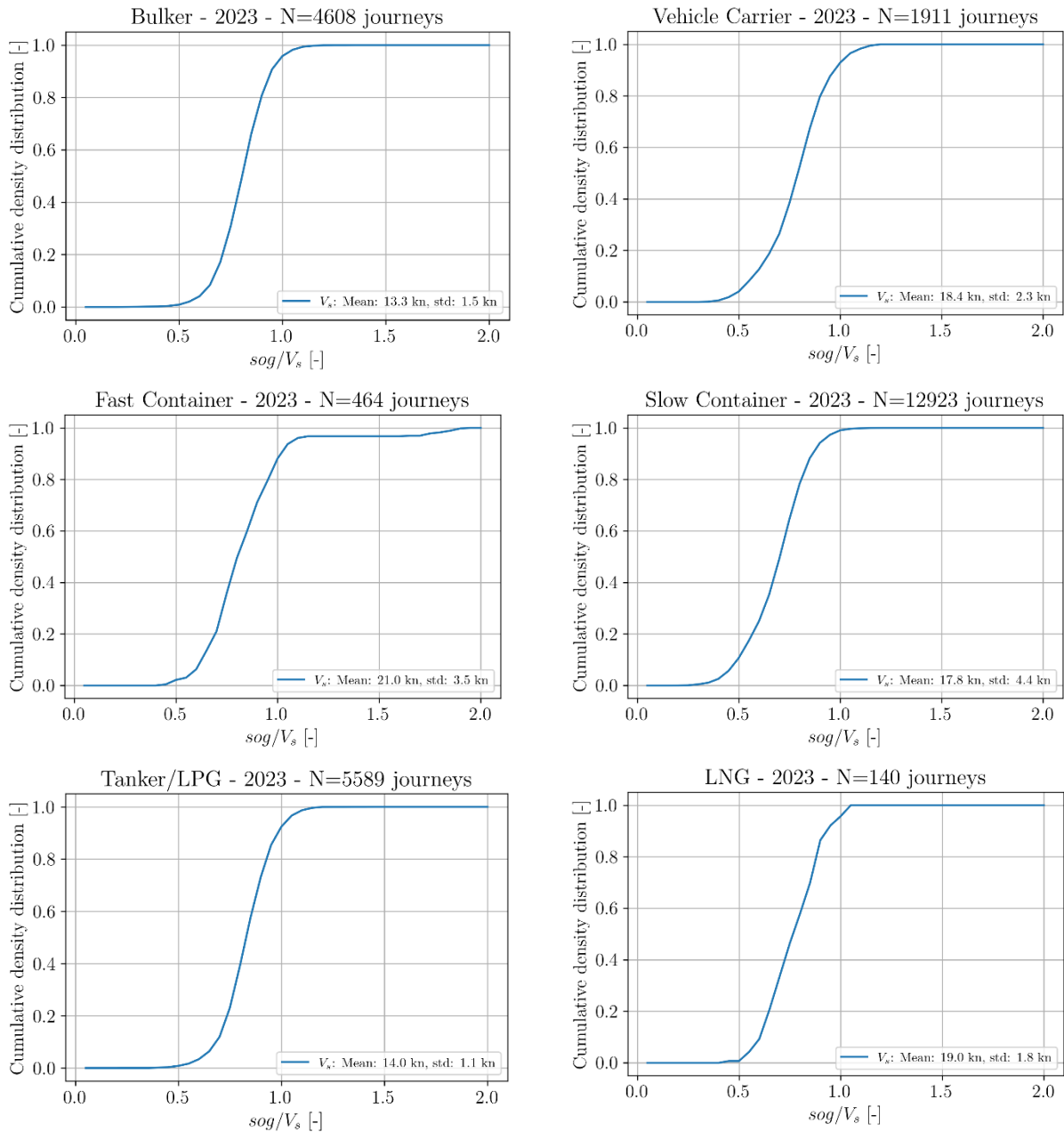


Figure A1-2 - Cumulative density distribution of the speed over ground normalised by the service speed per ship type. Bin width of 0.05.



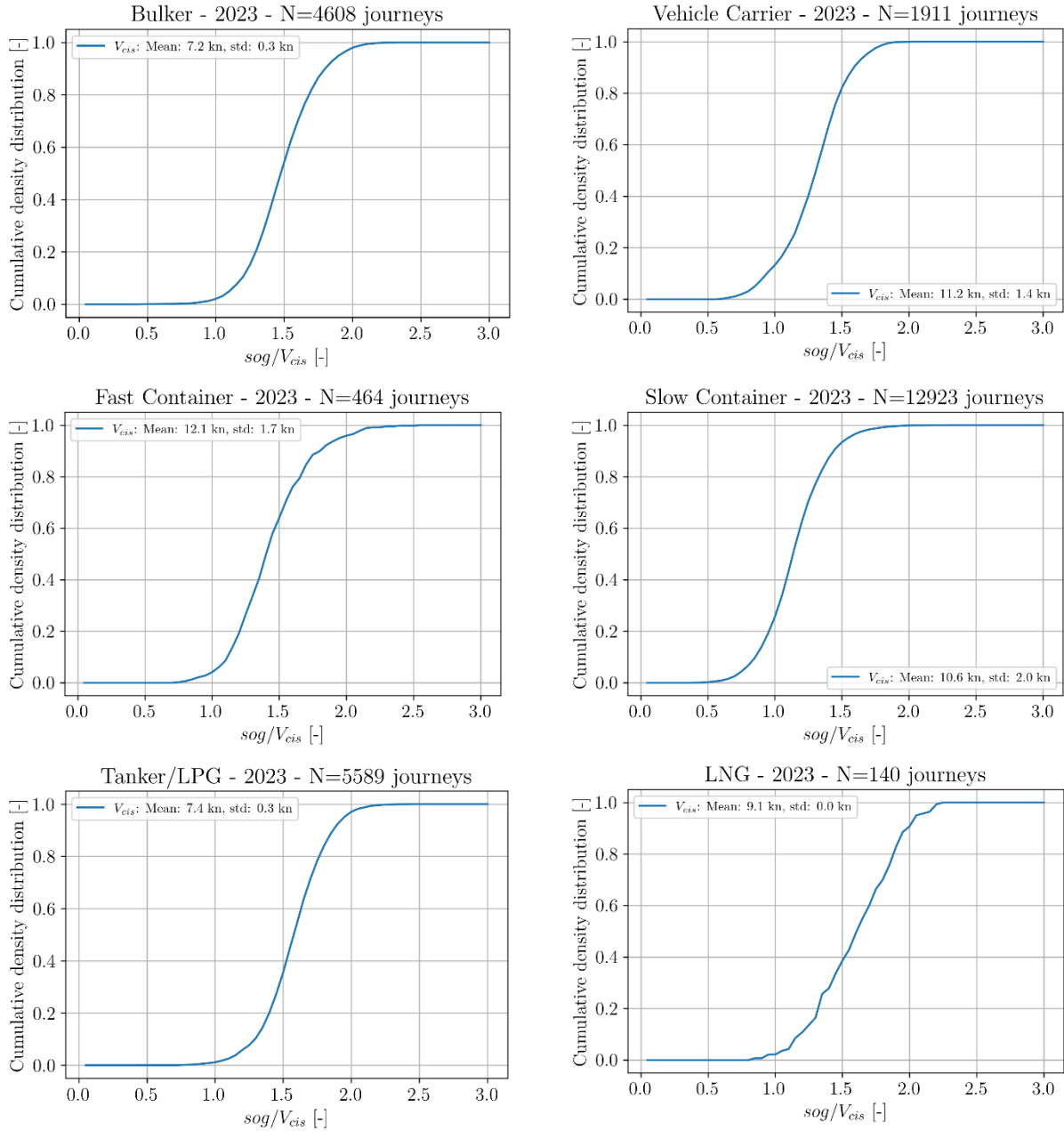


Figure A1-3 - Cumulative density distribution of the speed over ground normalised by the cavitation inception speed per ship type. Bin width of 0.05.

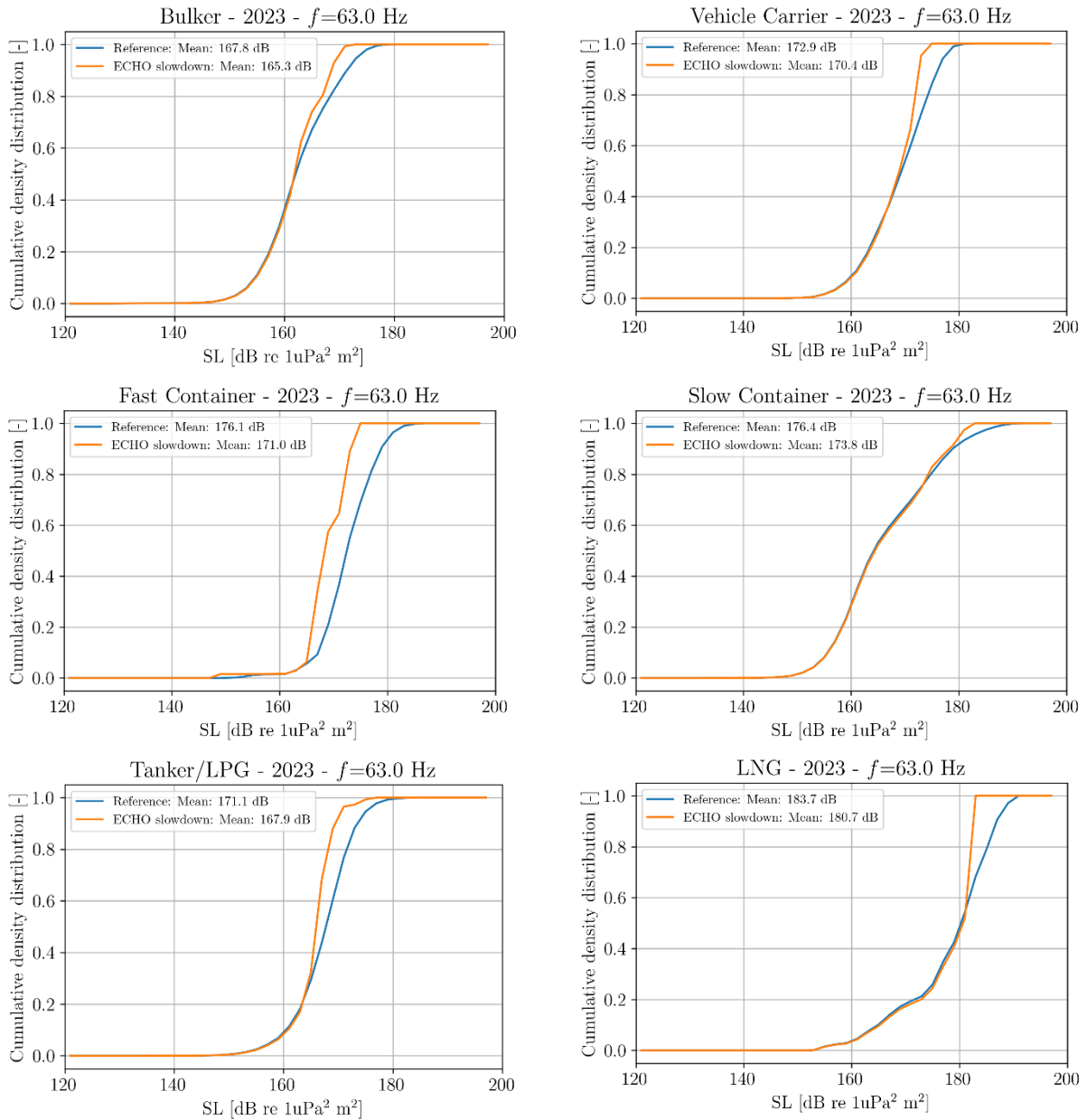


Figure A1-4 - Cumulative density distribution of the source levels for each ship category for a centre decade band of 63 Hz for two cases: reference and ECHO slowdown. The source level is estimated based on the J-E model. Bin width of 2 dB.

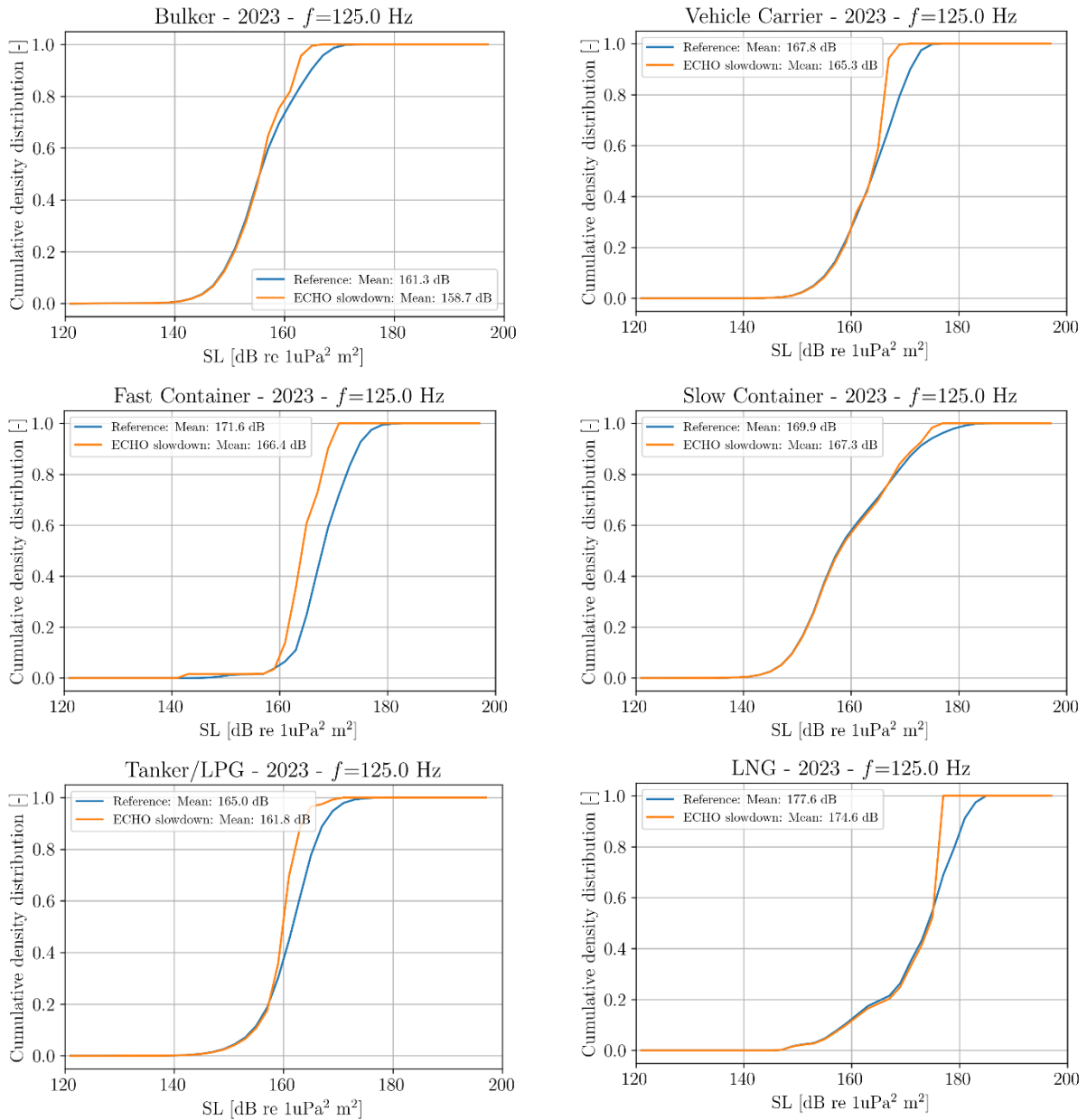


Figure A1-5 - Cumulative density distribution of the source levels for each ship category for a centre decade band of 125 Hz for two cases: reference and ECHO slowdown. The source level is estimated based on the J-E model. Bin width of 2 dB.

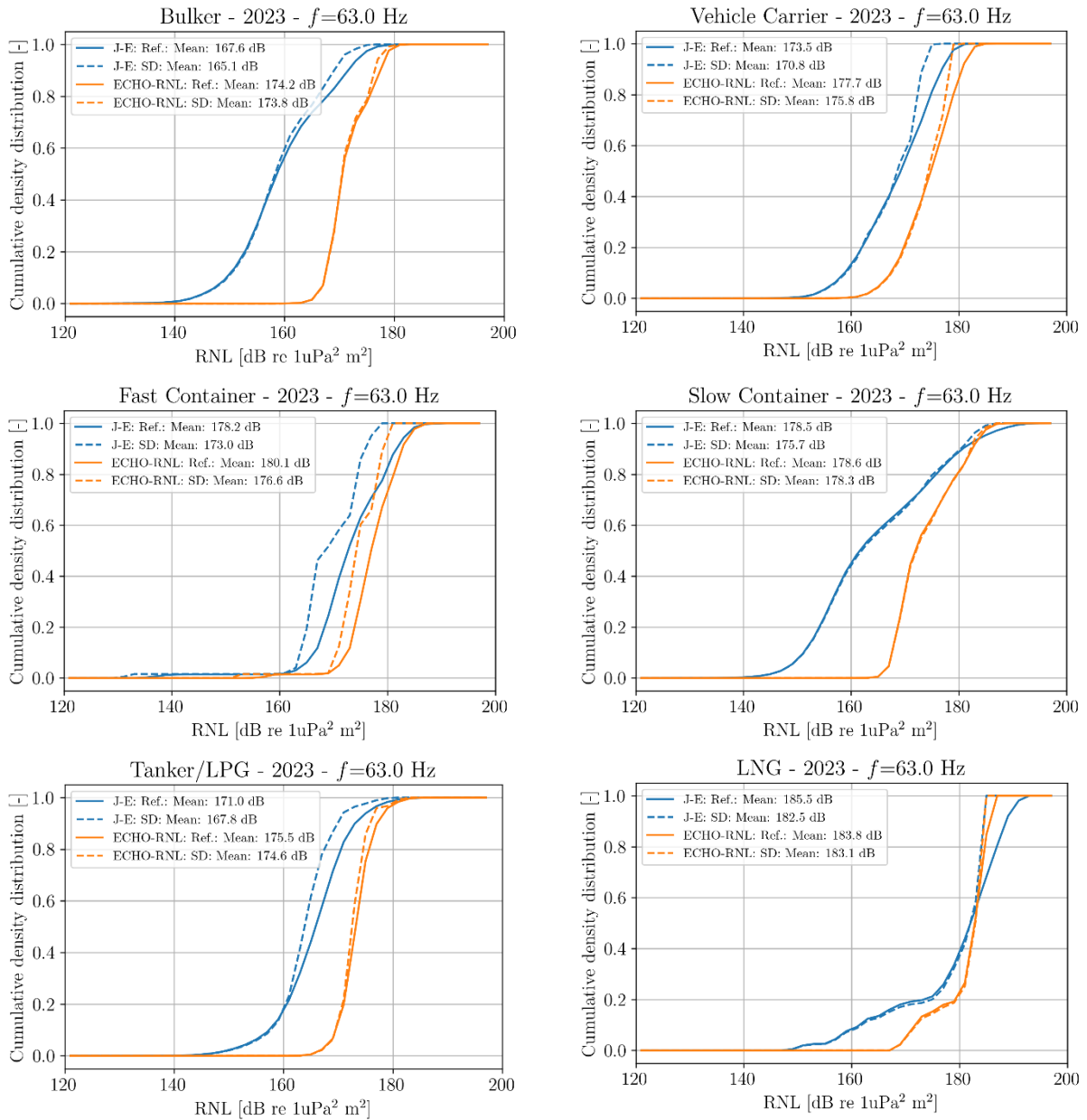


Figure A1-6 - Cumulative density distribution of the source levels for each ship category for a centre decade band of 63 Hz for two cases: reference and ECHO slowdown. The source levels are estimated based on the J-E model and the ECHO-RNL model. Bin width of 2 dB.

Table A1-1 - ORNEL and  $ORNL_{avg}$  (overall  $RNL_{avg}$ ) based on the estimates from the J-E model for the reference and slowdown cases. The overall level was calculated for decidecade bands from 20 Hz to 20 kHz.

	Reference	Slowdown	Reference	Slowdown
Ship type	ORNEL	ORNEL	$ORNL_{avg}$	$ORNL_{avg}$
	1 year, all data points	1 year, all data points	1 second, all data points	1 second, all data points
	[dB]	[dB]	[dB]	[dB]
<b>Bulker</b>	255.0	252.7	180.0	177.7
<b>Fast container</b>	254.6	250.1	179.6	175.1
<b>LNG</b>	253.9	251.2	179.0	176.3
<b>Slow container</b>	269.1	266.5	194.1	191.5
<b>Tanker/LPG</b>	258.2	255.3	183.2	180.4
<b>Vehicle carrier</b>	256.5	254.2	181.5	179.2

Table A1-2 - ORNEL and  $RNL_{avg}$  (overall  $RNL_{avg}$ ) based on the estimates from the ECHO-RNL model for the reference and slowdown cases. The overall level was calculated for decidecade bands from 20 Hz to 20 kHz.

	Reference	Slowdown	Reference	Slowdown
Ship	ORNEL	ORNEL	$ORNL_{avg}$	$ORNL_{avg}$
	1 year, all data points	1 year, all data points	1 second, all data points	1 second, all data points
	[dB]	[dB]	[dB]	[dB]
<b>Bulker</b>	259.8	259.3	184.8	184.3
<b>Fast container</b>	255.9	252.8	180.9	177.8
<b>LNG</b>	251.6	251.2	176.6	176.2
<b>Slow container</b>	268.8	268.3	193.9	193.3
<b>Tanker/LPG</b>	261.2	260.8	186.2	185.8
<b>Vehicle carrier</b>	258.7	257.0	183.7	182.0

MARIN  
P.O. Box 28

6700 AA Wageningen  
The Netherlands

T +31 317 49 39 11  
E [info@marin.nl](mailto:info@marin.nl)

I [www.marin.nl](http://www.marin.nl)  
   